Turkish Journal of Earth Sciences

Volume 29
Number 8 *SI-1*

Article 5

1-1-2020

Late Eocene to Early Oligocene palynostratigraphy of the Western Black Sea, EasternParatethys

RECEP HAYRETTİN SANCAY

ZÜHTÜ BATI

TÜBİTAK

Turkish Journal of Earth Sciences

http://journals.tubitak.gov.tr/earth/

Research Article

Turkish J Earth Sci
(2020) 29: 115-138

doi:10.3906/yer-1905-10

Late Eocene to Early Oligocene palynostratigraphy of the Western Black Sea, Eastern Paratethys

Recep Hayrettin SANCAY*, **Zühtü BATI**
Research and Development Center, Turkish Petroleum Corporation (TPAO), Ankara, Turkey

Received: 15.05.2019 • **Accepted/Published Online:** 30.10.2019 • **Final Version:** 02.01.2020

Abstract: The Eastern Thrace and Western Black Sea basins provide unique perspectives on the palaeogeographic reconstructions of the Paratethys. Although very thick and extensive Oligocene outcrops and well sections exist in the Thrace Basin, only a few comparable sections are available in the Black Sea onshore areas. In this study, five measured stratigraphic sections of Eocene to Oligocene age from the margins of the Western Black Sea were studied and palynomorph assemblages were identified quantitatively. Index dinoflagellate cyst events and a palynological biozonation as established in the Mediterranean were applied successfully. Priabonian units contain the Aal biozone, whereas Rupelian successions were represented by the Adi, Rac, Cin, and Hpu zones. Palynological analyses suggest that the youngest interval of the studied sections, the highest sample of Karaburun (2) and the upper part of Servez Beach, sit just above the *Wetzeliella gochtii* interval and are early-middle Rupelian in age (Cin and Hpu zones). The Karaburun (1) and the lower part of the Servez Beach sections represent *W. gochtii*-bearing intervals and are interpreted as early Rupelian in age (Rac, Cin, and Hpu zones). The Servez Road Dam section occurs below the *W. gochtii* interval. It is characterized by common occurrences of *Glaphyrocysta semitecta* and interpreted as earliest Rupelian in age (Adi and Rac zones). Finally, the Sazlıbosna section lies below the *Glaphyrocysta semitecta* zone and represents the oldest stratigraphic unit of the studied intervals. It yielded Eocene dinoflagellates such as *Areoligera taulomasentosa*, *Areosphaeridium michoudii*, *Rhombodinium perforatum*, *Homotryblium pallidum*, and *Stoveracysta ornata* and is interpreted as late Priabonian in age (Aal zone). Both palynomorph assemblages and organic matter constituents reflect shallow to open marine and nutrient-rich depositional conditions that occurred during Late Eocene–Early Oligocene time. The dominance of marine palynomorphs, without any indication of fresh water influx, might suggest that deposition took place before the isolation of the Paratethys, when the Western Black Sea region was still part of the Western Tethys during the earliest Oligocene (NP21–23).

Key words: Black Sea, Paratethys, Eocene, Oligocene, palynology

1. Introduction

The Eocene-Oligocene transition, with its significant record of climate change, has received much attention (e.g., Miller et al., 1991, 2008, 2009; Zachos et al., 1994, 2001; Diester-Haass and Zahn, 2001; van Mourik et al., 2001; Yancey et al., 2002; Bodiselitsch et al., 2004; Pagani et al., 2005; Sluijs et al., 2005; Alegret et al., 2008; Pearson et al., 2008; Schouten et al., 2008; Sotak, 2010; Sliwinska and Heilmann-Clausen, 2011; Houben et al., 2012). The Middle Eocene–Recent Thrace and Late Cretaceous–Recent Western Black Sea basins have unique palaeogeographical significance in having geological records not only of climate change but also of the closure of the Western Tethys and the formation of Paratethyan basins during the Late Eocene to Early Oligocene. Therefore, several biostratigraphical and palaeogeographical studies have focused on Eocene-Oligocene sediments in these locations (e.g., İslamoğlu et al., 2008; Less et al., 2011; Şafak and Güldürek, 2016; Gürgey and Batı, 2018; Kostopoulou et al., 2018; Özcan et al., 2018; Okay et al., 2019, 2020; Simmons et al., 2020).

In contrast to the opening of the Western Black Sea basin as a back-arc basin during the Late Cretaceous (Nikishin et al., 2015), the Thrace Basin is classified as a fore-arc basin related to the subduction of the Intra-Pontide Ocean (Görür and Okay, 1996), and it has Middle Eocene to Miocene sedimentary successions more than 9 km thick (Turgut et al., 1991). These units were divided into 5 depositional sequences in terms of different facies and sedimentary geometry due to faulting and sea-level fluctuations by means of outcrop, well log, core, seismic, and palaeontological data (Turgut and Eseller, 2000). Eocene units (represented by the clastic Karaağaç, Fıçıtepe, Gaziköy, Keşan, Koyunbaba, and Hamitabat formations and the carbonate Soğucak Formation) and Oligocene units (represented by the Ceylan, Danişmen, and Osmancık formations) crop out in several places in

* Correspondence: hsancay@tpao.gov.tr

the Thrace Basin (Siyako, 2006). However, there are only a few sections on the Turkish margins of the Western Black Sea containing Oligocene successions that can be studied palynologically for biostratigraphical purposes.

2. Geological setting

The Western Black Sea area is located in the central part of the Rhodope-Pontides fragment (Şengör and Yılmaz, 1981) and bounded by the İstanbul Zone in the east and the Rhodope-Strandja Massif in the west (Okay and Tüysüz, 1999; Okay, 2016). The İstanbul Zone is mainly represented by a Neoproterozoic-Cambrian crystalline basement, overlain by a Palaeozoic sedimentary sequence, the lowermost Triassic red beds, Lower Triassic shallow marine carbonates, Middle Triassic pelagic limestones, Upper Triassic turbidites (Turgut et al., 1991; Perinçek, 1991; Okay, 2016), and Upper Cretaceous to Palaeocene deep marine marly limestones (Özcan et al., 2012) in ascending order. The Rhodope-Strandja Massif, on the other hand, mainly comprises Upper Carboniferous to Permian metamorphic and granitic rocks (Okay, 2016), unconformably overlain by Triassic-Jurassic clastics and carbonates, Cenomanian sandy limestones, and Senonian volcanic and volcaniclastic rocks (Okay et al., 2001). Eocene and younger sediments unconformably overlie the older units following the Late Cretaceous tectonic juxtaposition of the İstanbul Zone and Rhodope-Strandja Massif in the Western Black Sea (Okay, 2016).

Mediterranean and intracontinental Paratethys basins occurred as new marine realms after the deformation of the Western Tethys Ocean due to the collision of India and Asia in the Late Eocene (Rögl, 1999). As a result of the orogeny of the Alpine thrust belt in the Late Eocene (Rögl, 1999), the Oligocene is represented mainly by a time of isolation in the Paratethys basins and favours Black Sea-type anoxic conditions. Even though marine conditions prevailed during Oligocene sedimentation in the Mediterranean, fluctuations in marine connections and thus strong provincialism/endemism mainly control the deposition of those successions in the Paratethys basins. The first record of the isolation (reflected by reduced salinity, brackish water, anoxic conditions, and deposition of black shales) occurred in the Solenovian (Early Oligocene) nannofossil biozone NP23 (e.g., Rögl, 1999; Schulz et al., 2005; İslamoğlu et al., 2008; Gürgey and Batı, 2018).

Palaeogeographically, the Thrace and the Western Black Sea regions were part of the Eastern Paratethyan Realm (Popov et al., 2004; İslamoğlu et al., 2008; Sachsenhofer et al., 2009) during the Eocene-Oligocene transition. The isolation of the Eastern Paratethys from the Tethys Ocean during the early Rupelian (Pshekhian chronostratigraphic unit of the Eastern Paratethys, NP21/22, to Solenovian unit NP23) resulted in the formation of the Thrace and Western Black Sea subbasins (Popov et al., 1993; Rögl, 1998). However, the presence of manganese ore deposits both in the Thrace Basin (Öztürk and Frakes, 1995; Gültekin, 1998) and Eastern Paratethys (Stolyarov and Ivleva, 1999; Varentsov, 2002; Varentsov et al., 2003) in the early Solenovian (early Rupelian), together with the presence of Early Oligocene oils generated from Lower Oligocene marine source rocks having similar geochemical characteristics in the Thrace Basin and in Western Turkmenistan (Gürgey, 2007), might suggest that the seaway connection was still open between Thrace and the Eastern Paratethys through the Western Black Sea in the early Rupelian. According to Özcan et al. (2018), the marine connection between these two basins was established in the Priabonian and existed during the Late Eocene to Early Oligocene via the Çatalca gap, west of İstanbul (Okay et al., 2019a). This marine connection was then closed during the middle Early Oligocene (Okay et al., 2019a).

3. Materials and methods

A total of 36 samples were obtained from 4 different sections of the western coast of the Black Sea (Figure 1). However, only 12 of these were fossiliferous and yielded abundant, well-preserved palynomorphs and were thus taken into consideration for biostratigraphical interpretations. Following disaggregation and cleaning, samples were processed by a standard palynological sample preparation technique of demineralisation with hydrochloric acid (HCl) and hydrofluoric acid (HF) followed by heavy-density liquid separation ($ZnCl_2$). After sieving at 200 μm and 10 μm, samples were mounted in glycerine jelly for microscope studies. All of the productive samples were analysed quantitatively and then the percentages of each taxon and palynomorph assemblages were calculated (see Appendix). Studied materials are stored in the Palynology Laboratory Archive of the Turkish Petroleum Corporation Research and Development Center in Ankara, Turkey.

4. Studied sections

All of the studied sections are located in the Western Black Sea region (Figure 1) and composed mainly of marl with subordinate conglomerate, sandstone, siltstone, and claystone interfingering with limestone, and some volcanosedimentary deposits (tuff) (Figures 2–6).

4.1. Karaburun

A total of 11 samples were collected from two sections from the Karaburun region. Seven samples were collected from the Karaburun (1) section (GPS coordinates: 41°20′51″61N, 28°40′47″71E) (Figure 2). This section, on Cape Karaburun, features well-known outcrops that encompass the Eocene-Oligocene succession on the

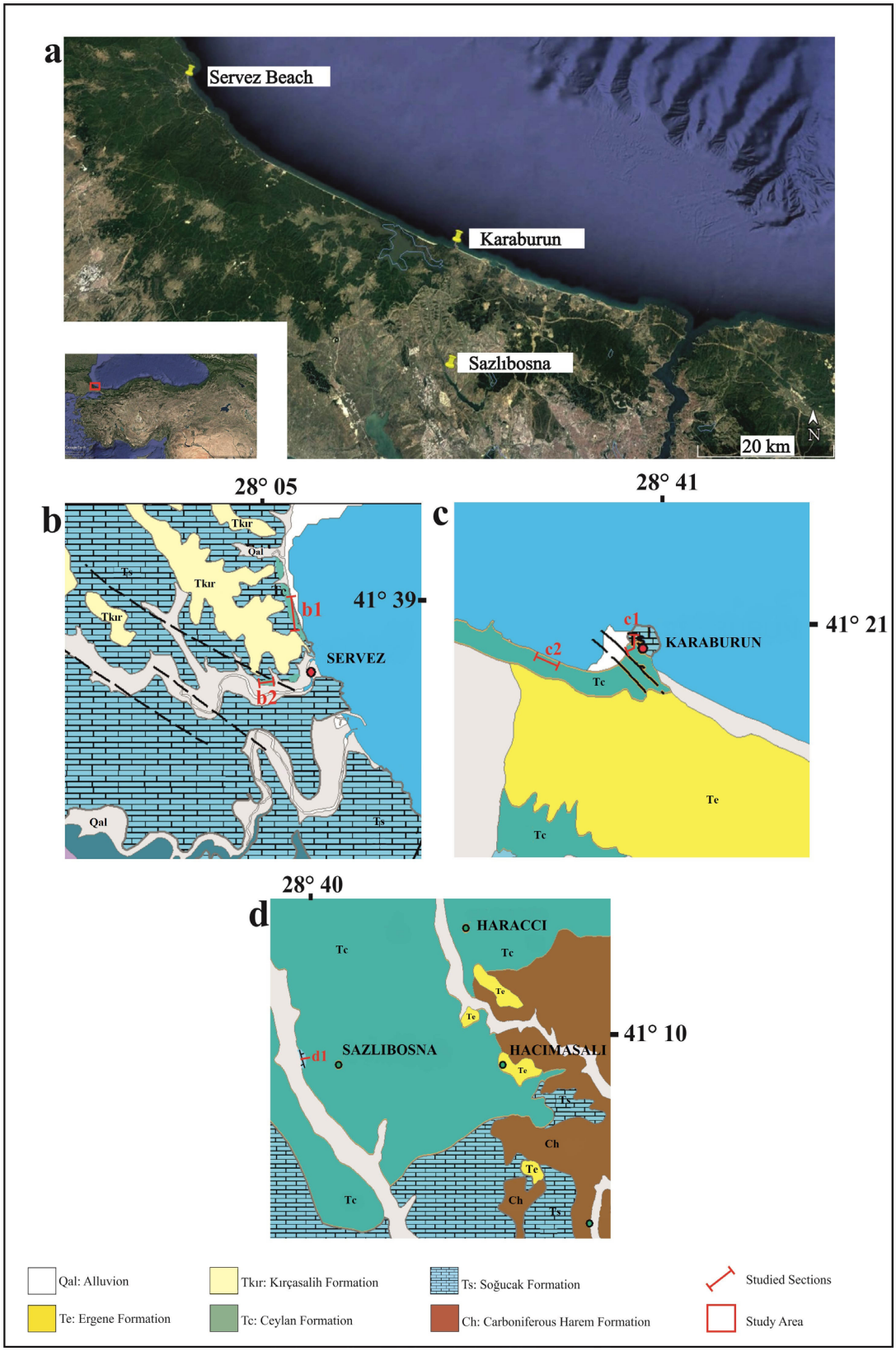

Figure 1. Location map (a) and geological maps (b–d) of the studied sections (b1: Servez Beach section, b2: Servez Road Dam section, c1: Karaburun (1) section, c2: Karaburun (2) section, d1: Sazlıbosna section).

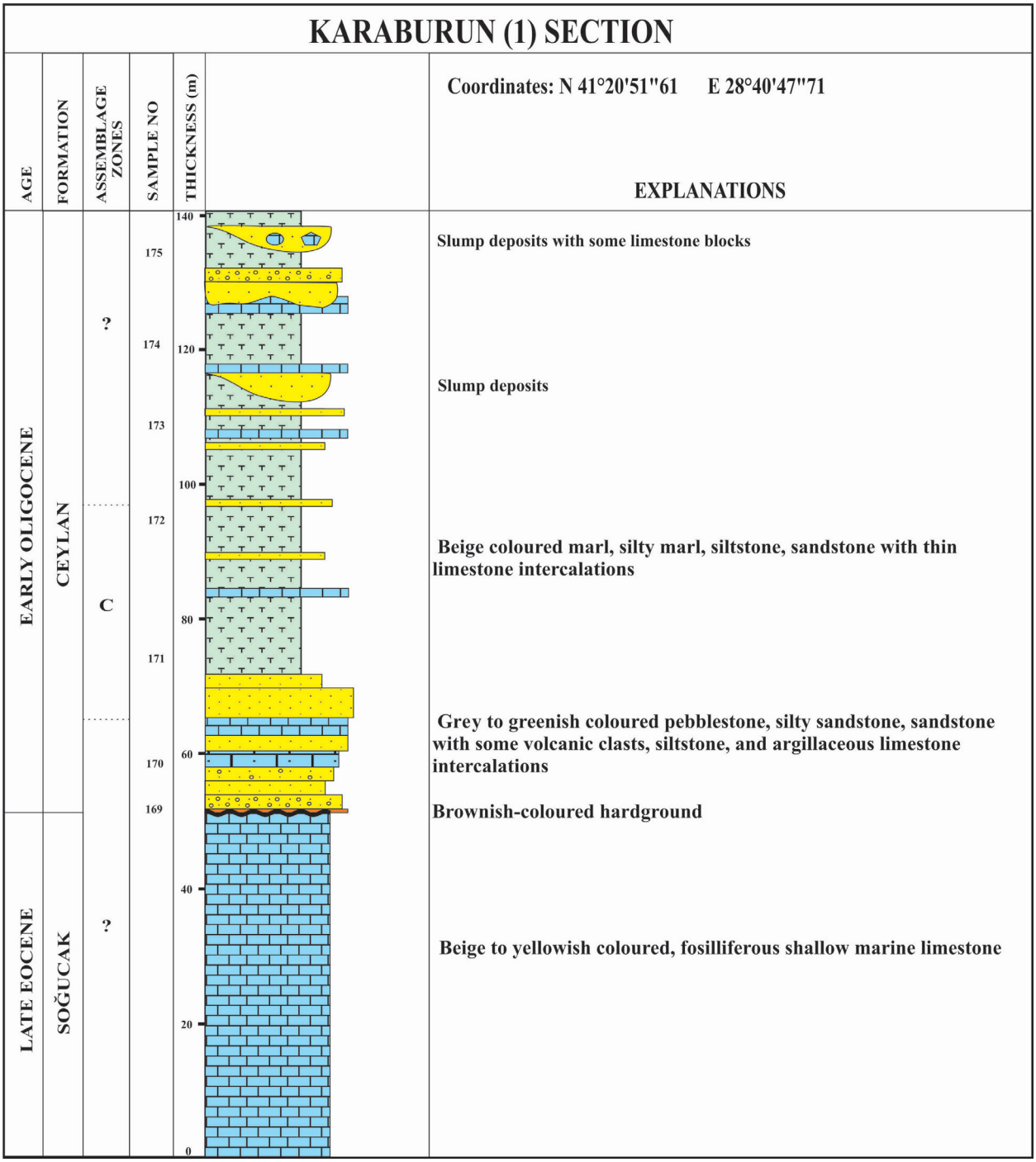

Figure 2. Stratigraphic section of Karaburun (1) and the sample locations.

Thracian coast of the Western Black Sea (Less et al., 2011; Okay et al., 2019; the "Footwall Section" described by Simmons et al., 2020). The Karaburun (1) section is about 140 m thick and comprises conglomerate, sandstone, calcareous sandstone, siltstone, mudstone, marl, silty marl, shale, and bioclastic limestone. The Upper Eocene shallow marine limestones of the Soğucak Formation at the base are unconformably overlain by the Lower Oligocene Ceylan Formation composed of shallow marine calcareous sandstone, siltstone, conglomerate, and deeper marine marls. Okay et al. (2019) and Simmons et al. (2020) used the local term "İhsaniye Formation" for this rock unit based on its distinctive lithological character. We prefer the term "Ceylan Formation" to permit ready

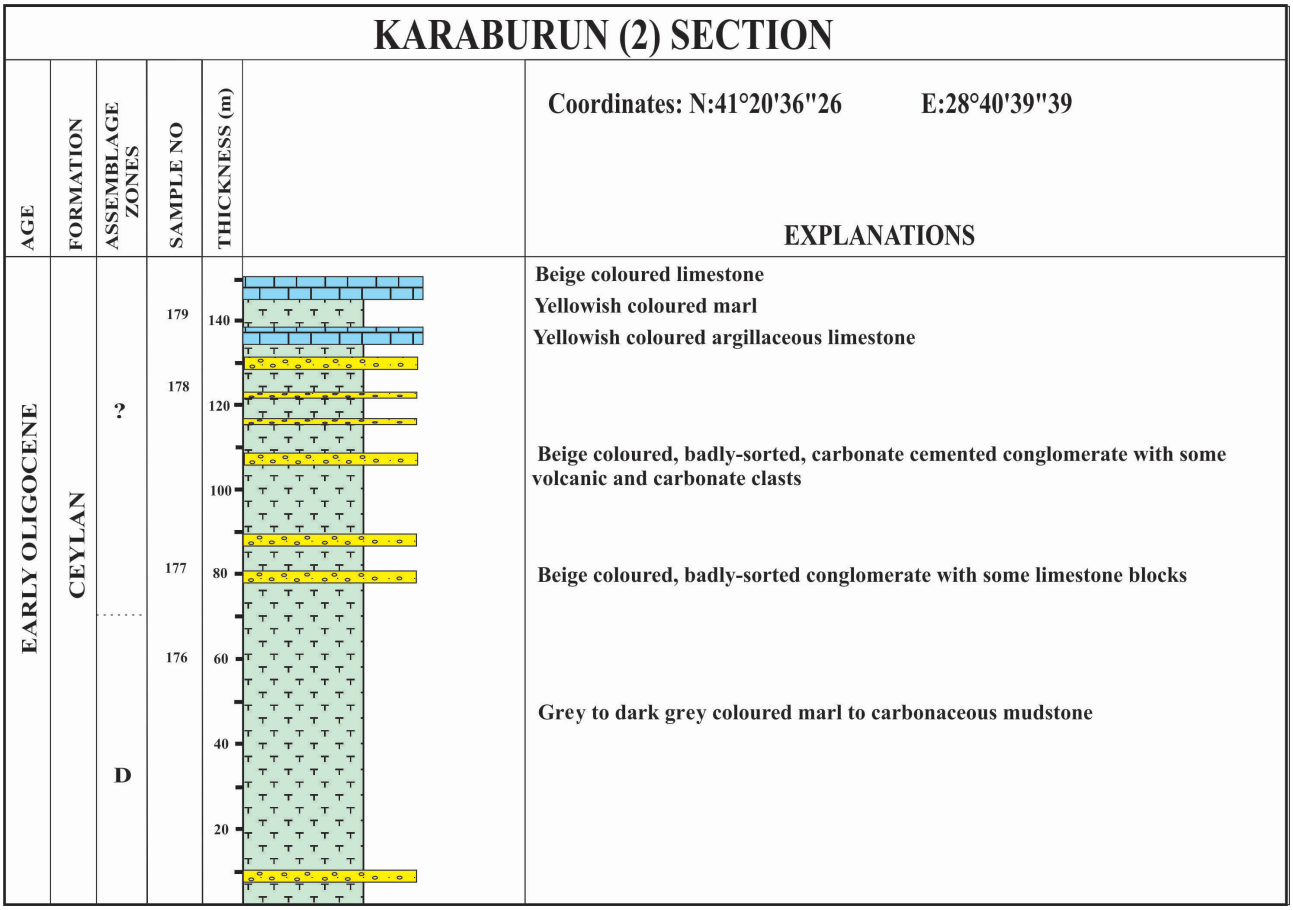

Figure 3. Stratigraphic section of Karaburun (2) and the sample locations. See also Simmons et al. (2020).

correlation with the stratigraphy of the adjacent Thrace Basin. A late Priabonian age (SBZ20) was assigned for the Soğucak Formation in the Karaburun section by Okay et al. (2019), Yücel et al. (2020), and Simmons et al. (2020) based on benthic foraminifera. Simmons et al. (2020) have demonstrated that the section above the Soğucak Formation at Karaburun (1) is of Early Oligocene (NP23) (early Rupelian) age and represents transgression onto the footwall of a fault, while Oktay et al. (1992), Sakınç (1994), Gedik et al. (2014), and Okay et al. (2019) also reported an Early Oligocene age for these strata at Karaburun. While confirming an early Rupelian age, dinoflagellate assemblages recorded in our material (notably the presence of Assemblage Zone C with *Wetzeliella gochtii*) suggest that at least part of the section may be older than NP23 (Figure 7).

In contrast to the observations on the nature of the boundary between the Soğucak and Ceylan formations by Natalin and Say (2015), a clear unconformity surface with a hardground level between the Eocene and Oligocene successions has been observed in this section (Figures 2 and 7).

Four samples have been collected from the 150-m-thick Karaburun (2) section (GPS coordinates: 41°20′36″26N, 28°40′39″39E) to the west of the Karaburun (1) section. This is the "Hanging Wall Section" described in detail by Simmons et al. (2020) and Tulan et al. (2020). Marl, siltstone, and sandstone dominate this section with thin layers of limestone present towards the top (Figure 3). This section has been demonstrated by Simmons et al. (2020) to represent more complete Early Oligocene stratigraphy at Karaburun with nannoplankton biozones NP21–NP23 supported by planktonic foraminifera (Biozones O1–O2). Our limited number of samples appear to lie within the upper part of this age range (Assemblage Zone D).

4.2. Servez Beach

Ten samples have been obtained from the 128-m-thick Servez Beach section (GPS coordinates: 41°39′06″35N, 28°05′18″78E). This section mainly comprises conglomerate, sandstone, siltstone, claystone, mudstone, and shallow marine limestone layers (Figure 4) and has been extensively described by Okay et al. (2020). In our view, the transition between the carbonates of the Soğucak and the marls and clastics of the Ceylan formations

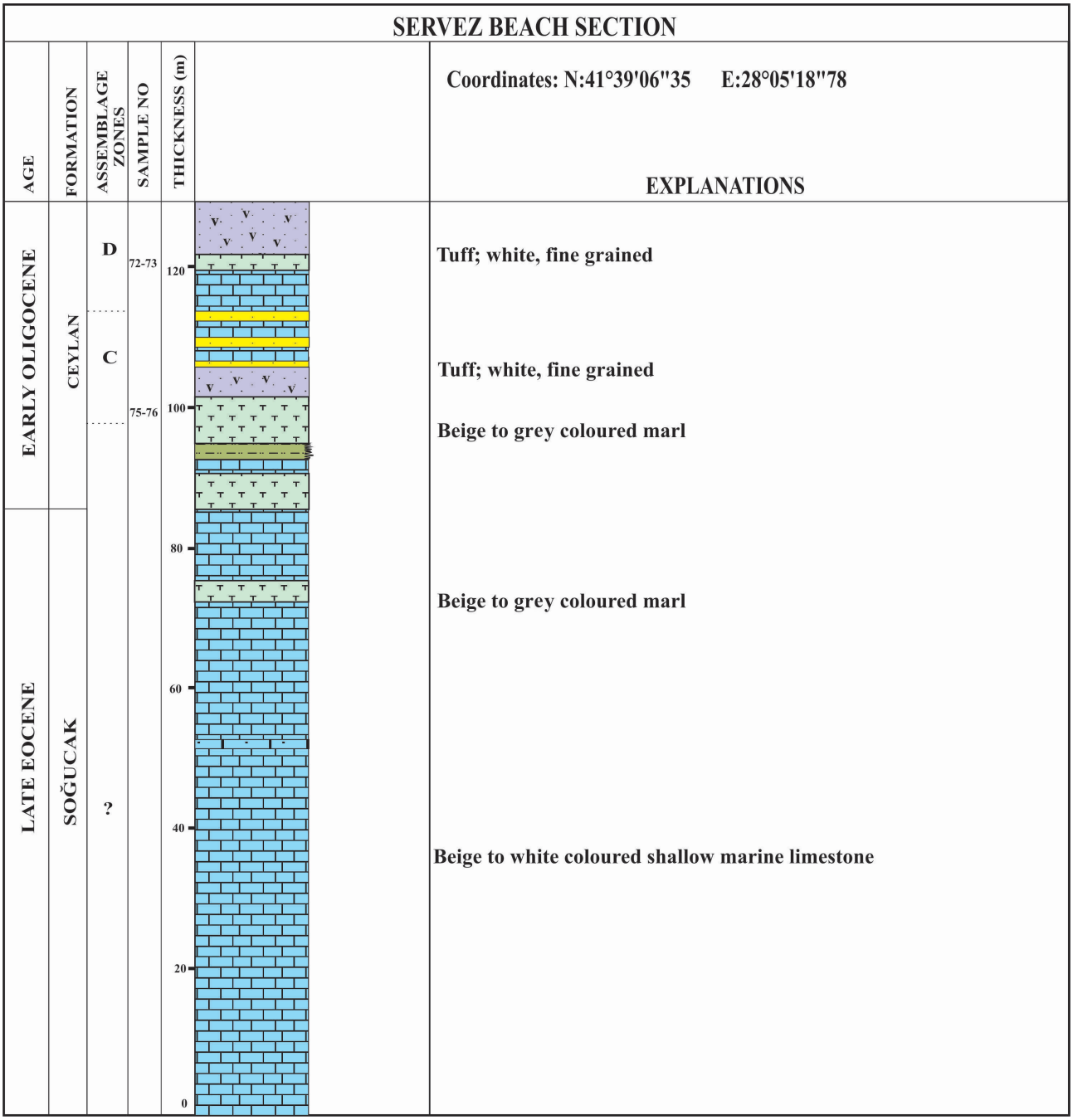

Figure 4. Stratigraphic section of Servez Beach and the sample locations. See also Okay et al. (2020).

(termed "Servez Formation" by Okay et al., 2020) seems to be gradational. Because of the unsuitable lithologies for the preservation of organic matter within the Soğucak Formation and the lack of samples from the basal part of the overlying Ceylan Formation, there is no palynological evidence in this study for the nature of the boundary and the contemporaneous sediments of NP21 studied by Simmons et al. (2020) at Servez Beach. From the base of the Ceylan Formation (palynologically unsampled interval), based on calcareous nannoplankton, larger benthic foraminifera, and radiometric ages derived from interbedded tuffs, Okay et al. (2020) also confirmed that the clastic succession above the Soğucak Formation at Servez Beach is low in the Early Oligocene (NP21). The first palynological record was obtained from 102 m in the Ceylan Formation (sample 76 in Figure 4) and suggests an early Rupelian age (NP22–23).

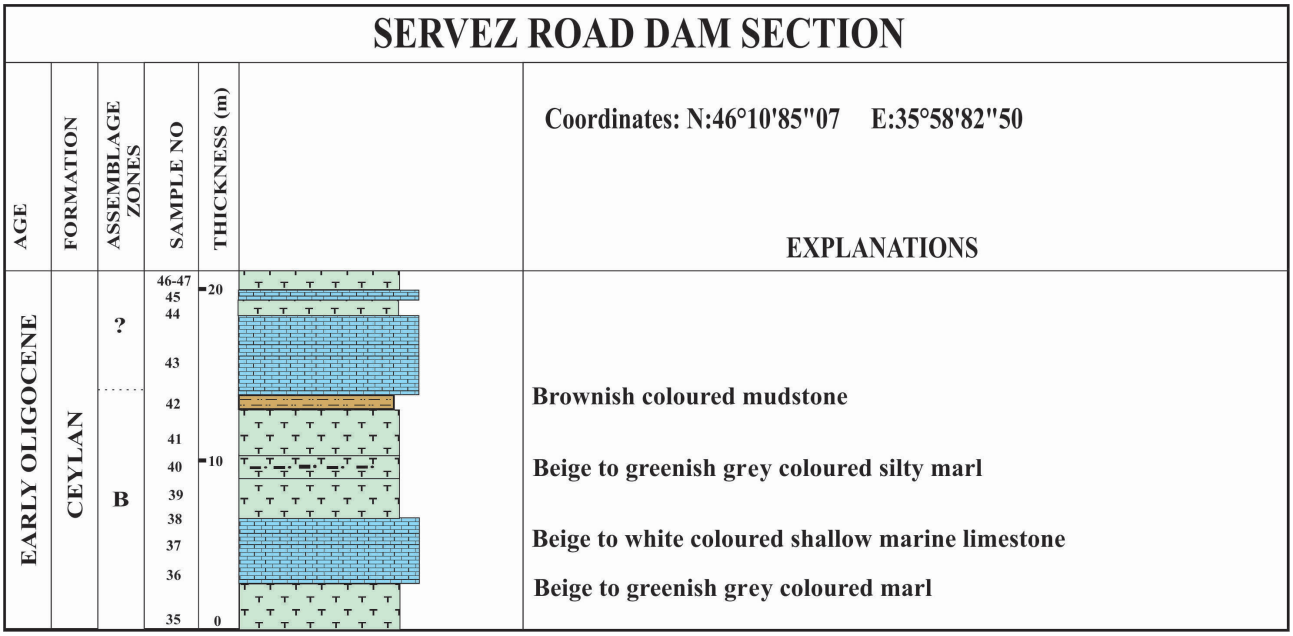

Figure 5. Stratigraphic section of Servez Road Dam and the sample locations.

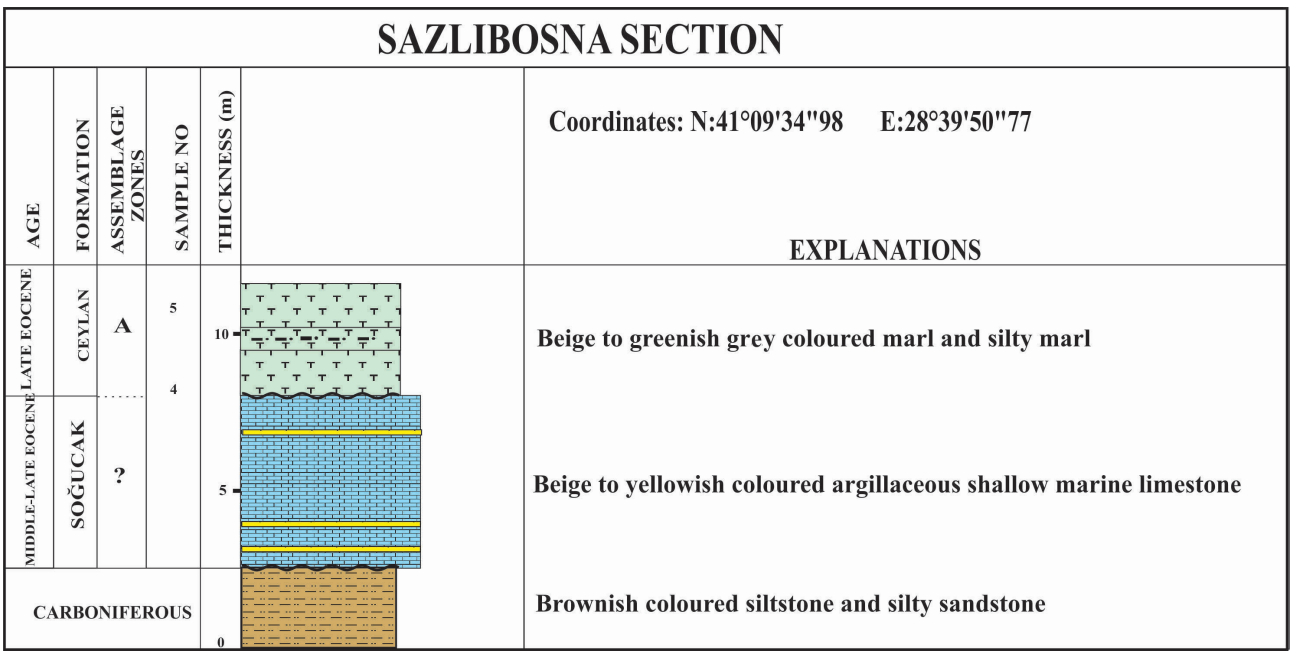

Figure 6. Stratigraphic section of Sazlıbosna and the sample locations.

The Soğucak Formation outcrop at Servez Beach was studied micropalaeontologically by Less et al. (2011) (the Kıyıköy Region in their study). They reported a Priabonian age (SBZ19–20) based on benthic foraminifera and two depositional facies for deposition of the Soğucak Formation. Shallow-water, high-energy, middle-shelf conditions dominated the lower part of the Soğucak Formation while low-energy, deeper middle-shelf conditions were observed towards the top (Less et al., 2011). A similar deepening trend has also been observed in this study, in which shallow-water limestones of the Soğucak Formation grade into marl and marl-limestone intercalations.

4.3. Servez Road Dam

The Servez Road Dam section is about 21 m thick and 13 samples were collected from the locality (GPS coordinates:

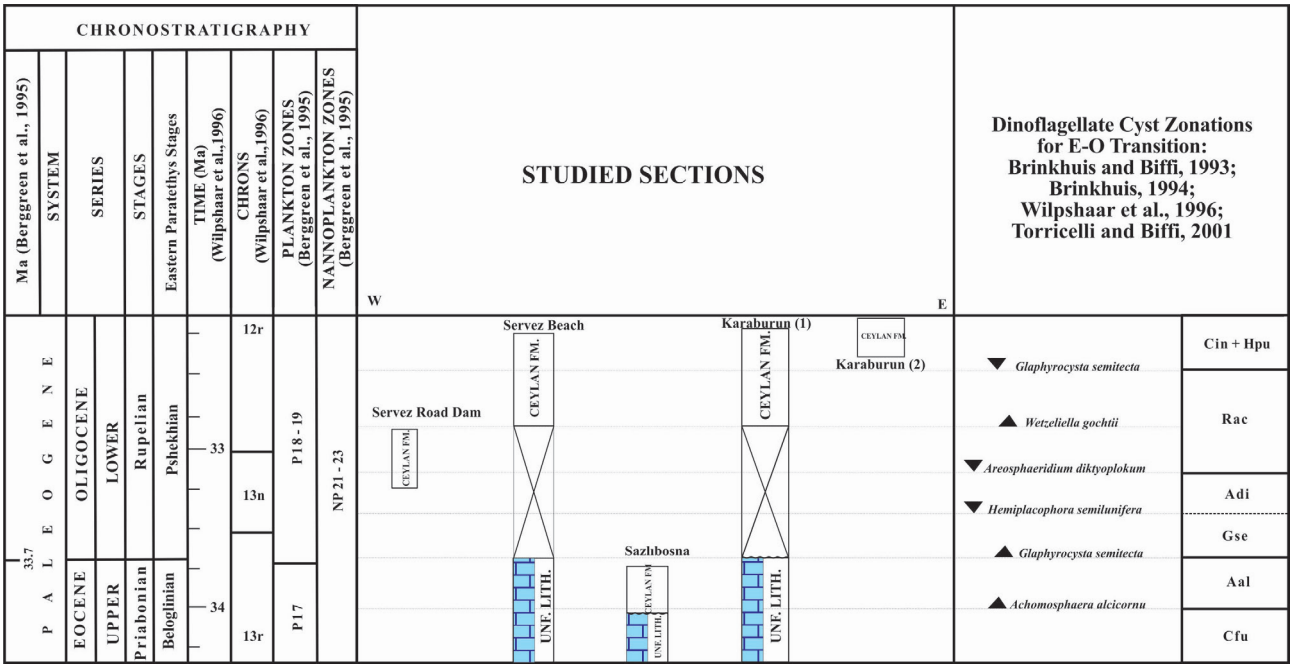

Figure 7. Biochronostratigraphic chart and the summary of dinoflagellate cyst zonations (Brinkhuis and Biffi, 1993; Brinkhuis, 1994; Wilpshaar et al., 1996; Torricelli and Biffi, 2001).

46°10′85″07N, 35°58′82″50E). Siliciclastic lithologies of sandstone, siltstone, mudstone, and marl dominate this section (Figure 5).

The last occurrence (LO) of *Areosphaeridium diktyoplokum* was recorded in this section (7-m level, Figure 5). This bioevent is stratigraphically important and draws the boundary between the Adi and Rac zones (Brinkhuis and Biffi, 1993; Brinkhuis, 1994; Wilpshaar et al., 1996; Torricelli and Biffi, 2001) in the earliest Rupelian.

Phthanoperidinium comatum, identified at the 12-m level in the Servez Road Dam Section, is another important taxon that might be indicative for the Rupelian (e.g., Liengjarern et al., 1980; Medus and Pairis, 1990). The LO of *Phthanoperidinium* spp. including *P. comatum* was reported in the NSO-3 zone of Simaeys et al. (2005) in the "early" Rupelian in the North Sea, in the "late" Rupelian in the lower part of NP23 in the Labrador Sea (Head and Norris, 1989), and in the early or middle Rupelian in Egypt (El Beialy et al., 2019).

4.4. Sazlıbosna

Two samples were derived from the 12-m-thick Sazlıbosna section (GPS coordinates: 41°09′34″98N, 28°39′50″77E). Carboniferous sandstone, siltstone, and slate are unconformably overlain by the Eocene limestones of the Soğucak Formation, which is then unconformably overlain by Oligocene siltstones and marls (Figure 6). An age close to the Middle-Late Eocene (Bartonian-Priabonian) boundary (SBZ18A) was determined for the Soğucak Formation in the Sazlıbosna section by Okay et al. (2019a) based on larger benthic foraminifera. Similar to the palynological results in this study, a late Priabonian age (P16–17 zones) was also assigned by Okay et al. (2019a) for the siliciclastics overlying the Soğucak Formation in the Sazlıbosna section based on planktonic foraminifera. The upper boundary of the Priabonian successions (top of the Aal zone of Brinkhuis and Biffi, 1993; Brinkhuis, 1994; Wilpshaar et al., 1996; Torricelli and Biffi, 2001), defined by the first occurrence (FO) of *Glaphyrocysta semitecta*, could not be detected palynologically in this section, suggesting that the studied interval is late Priabonian in age but is not the latest Priabonian (Figures 7 and 8).

The presence of *Areoligera tauloma-sentosa* at the 12-m level in the Sazlıbosna section is an important criterion for recognising the latest Priabonian. The Late Eocene (NP16/17) LO of *A. tauloma-sentosa* is a synchronous dinoflagellate cyst event (e.g., Costa et al., 1976 in England; Eldrett et al., 2004 in the Norwegian-Greenland Sea; Heilmann-Clausen and van Simaeys, 2005 in the Central Danish Basin). *Reticulatosphaera actinocoronata* and *Areoligera semicirculata* were also identified at the same level, confirming the late Priabonian age since their FOs were documented as 35.1 Ma and 33.73 Ma, respectively, in the late-latest Priabonian (Williams et al., 2004).

The presence of *Areosphaeridium michoudii* and *Stoveracysta ornata* was also determined at the 12-m level in the Sazlıbosna section. The LO of *A. michoudii* at 35.4 Ma in

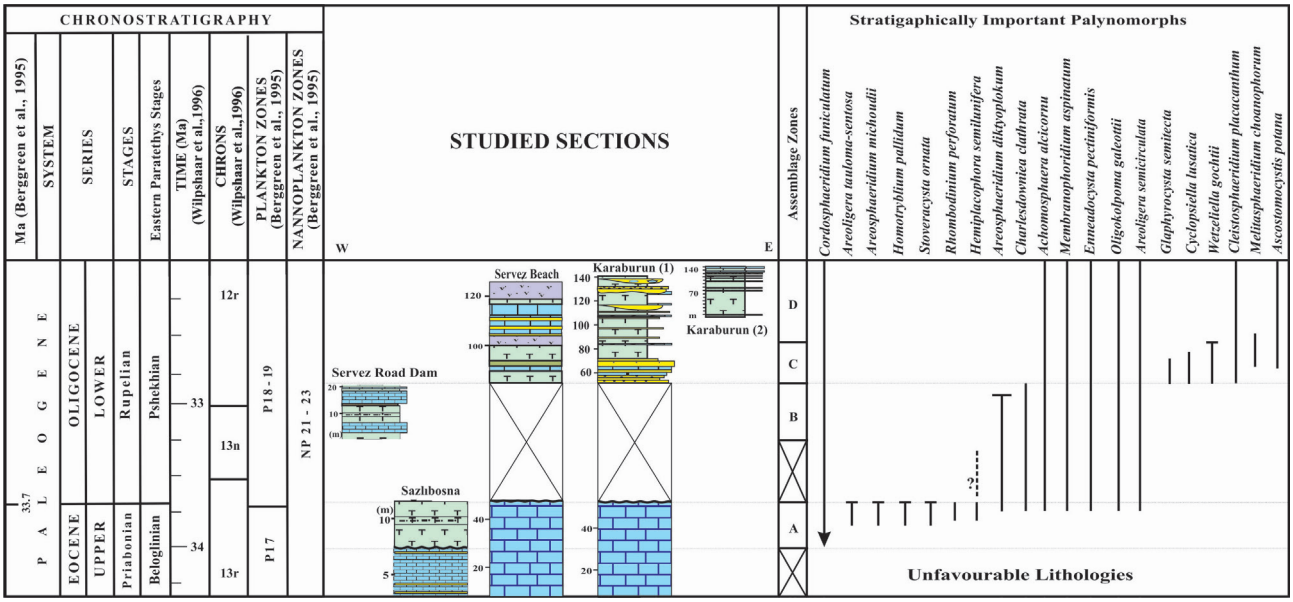

Figure 8. Biochronostratigraphic chart and stratigraphic occurrences of the selected palynomorphs.

the Late Eocene (NP19–20) was magnetostratigraphically calibrated in the Norwegian-Greenland Sea by Eldrett et al. (2004). The same event occurred in the latest Eocene in the NP19–20 zone in the Polish Carpathians (Gedl, 2004a, 2005). The Late Eocene (Priabonian) LO of *A. michoudii* was also reported from the Central Danish Sea (Heilmann-Clausen and van Simaeys, 2005) and North Sea (Bujak, 1994; Bujak and Mudge, 1994). The FO of *S. ornata* is another important dinoflagellate event for recognising the Priabonian (e.g., Brinkhuis and Biffi, 1993; Brinkhuis, 1994; Williams et al., 2004; van Mourik and Brinkhuis, 2005; Mahboub et al., 2019).

The presence of *R. actinocoronata* in the 12-m level in the Sazlıbosna section is noteworthy since the FO of *R. actinocoronata* was reported in the Cfu zone in the latest Late Eocene in Italy (Brinkhuis and Biffi, 1993; Coccioni et al., 2000) and implies ages not older than Late Eocene.

5. Palynostratigraphy

A total of 111 palynomorph species have been identified in four studied sections composed of 75 dinoflagellates; 1 acritarch; 32 spores, pollen, and fungi; and 3 other marine palynomorphs (foraminiferal linings, scolecodont, and *Tasmanites*). Distributions of the palynomorphs throughout the studied sections are provided in Figure 9. Percentages of each palynomorph taxon and digital images of some selected palynomorphs are documented in the Appendix and Figures 10–16, respectively.

The standard dinoflagellate cyst zonations of Brinkhuis and Biffi (1993), Brinkhuis (1994), Wilpshaar et al. (1996), and Torricelli and Biffi (2001) for the Mediterranean (Figure 7) were applied successfully in this study of Western Black Sea Upper Eocene-Lower Oligocene sediments. The lowermost relevant biozone in the Late Eocene is the Aal zone (late Priabonian), defined as an interval from the FO of *Achomosphaera alcicornu* to the FO of *Glaphyrocysta semitecta*. Early Oligocene zones are in the following ascending order: the Gse zone (earliest Rupelian), an interval from the FO of *G. semitecta* to the LO of *Hemiplacophora semilunifera*; the Adi zone (early Rupelian), an interval from the LO of *H. semilunifera* to the LO of *Areosphaeridium diktyoplokum*; the Rac zone (early Rupelian), an interval from the LO of *A. diktyoplokum* to the LO of *G. semitecta*; and the Cin zone (early-?middle Rupelian), an interval from the LO of *G. semitecta* to the FO of *Hystrichokolpoma pusillum*.

Four assemblage zones (Figure 8) were recognized in the studied material and these can be related to the biozones listed above. These units represent late Priabonian, earliest Rupelian, early Rupelian, and early-middle Rupelian intervals.

5.1. Assemblage Zone A

Age Assignment: Late Priabonian
Corresponding dinoflagellate zone: Aal (*Achomosphaera alcicornu*) zone
Corresponding planktonic foraminiferal zone: P17
Corresponding nannoplankton zone: NP21
Corresponding Eastern Paratethyan Regional Stage: Beloglinian
Samples: Sazlıbosna section (samples 4 and 5)
The samples in this interval occur below the *Glaphyrocysta semitecta* zone and are characterized by the presence of

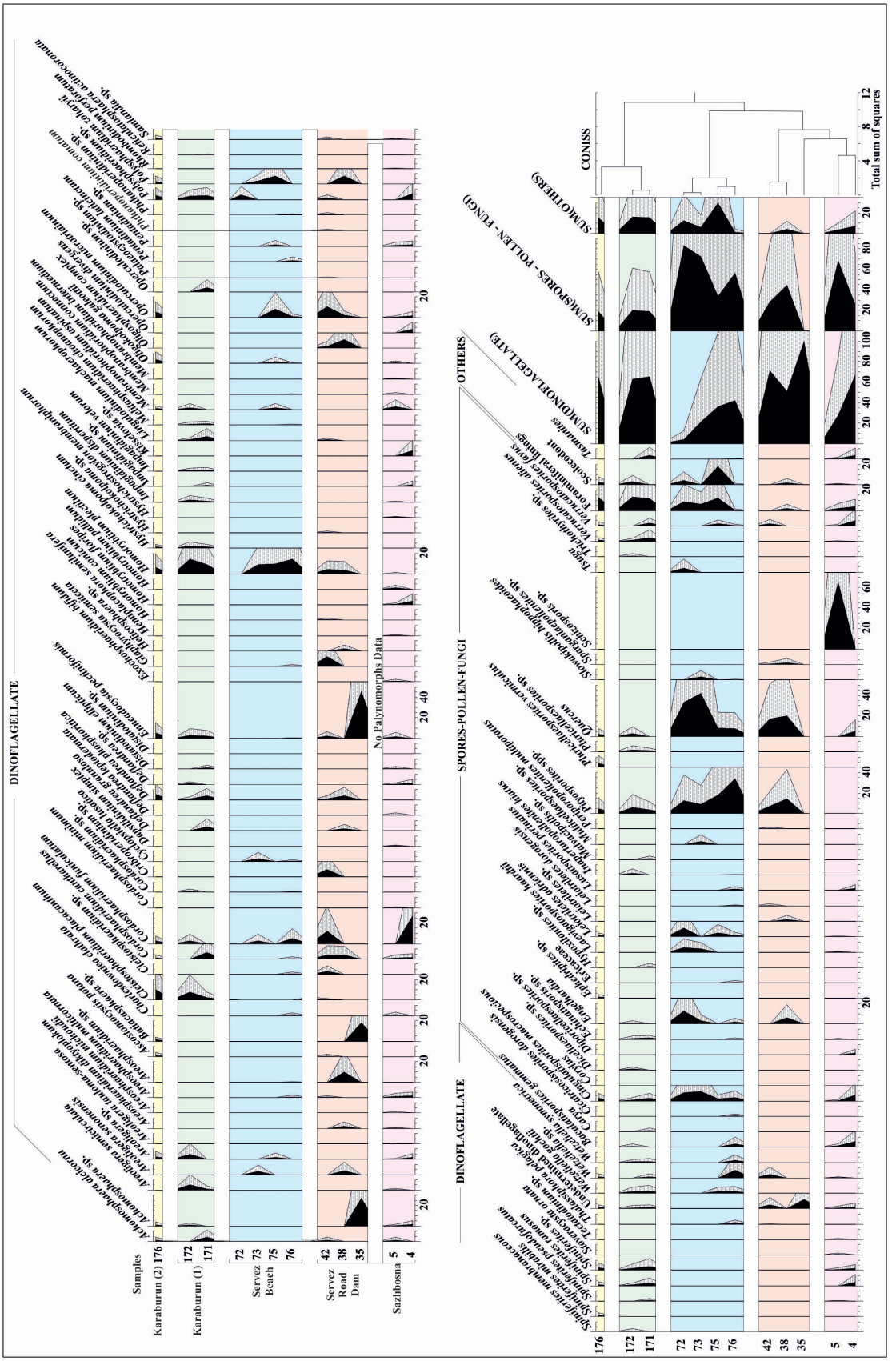

Figure 9. Distribution of palynomorphs and palynomorph groups in the studied sections.

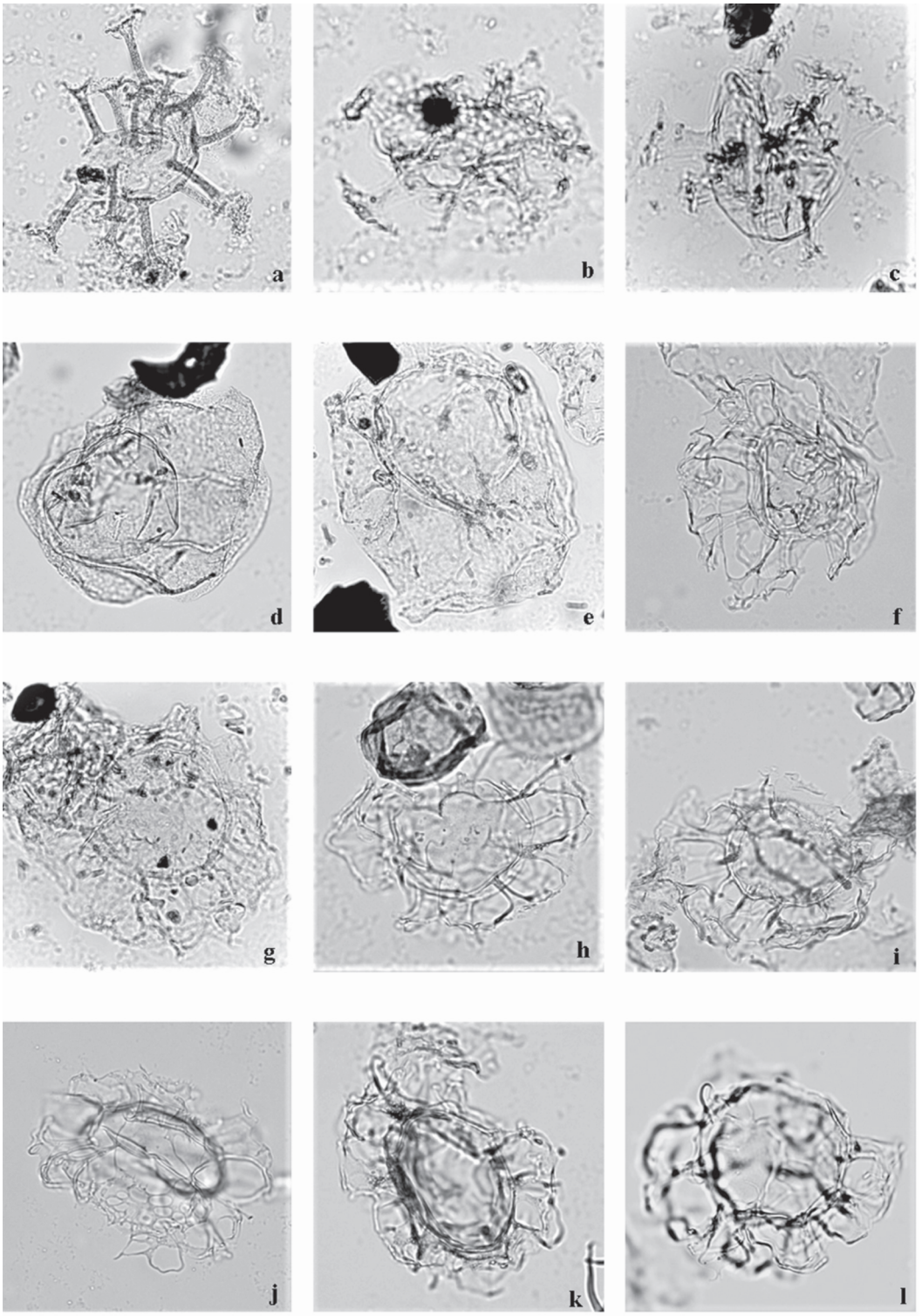

Figure 10. a) *Areosphaeridium diktyoplokum* (Sazlıbosna section; Sample No. 5; 93.79 μm); b) *Reticulatosphaera actinocoronata* (Sazlıbosna section; Sample No. 5; 31.03 μm); c) *Oligokolpoma galeottii* (Sazlıbosna section; Sample No. 5; 41.37 μm); d) *Thalassiphora pelagica* (Servez Road Dam section; Sample No. 42; 83.44 μm); e) *Thalassiphora pelagica* (Servez Beach section; Sample No. 76; 79.31 μm); f) *Glaphyrocysta semitecta* (Servez Road Dam section; Sample No. 42; 54.48 μm); g) *Glaphyrocysta semitecta* (Servez Beach section; Sample No. 76; 63.44 μm; h) *Glaphyrocysta semitecta* (Servez Road Dam section; Sample No. 42; 59.31 μm); i) *Glaphyrocysta semitecta* (Servez Road Dam section; Sample No. 42; 60.68 μm); j) *Glaphyrocysta semitecta* (Servez Road Dam section; Sample No. 42; 60.00 μm); k) *Glaphyrocysta semitecta* (Servez Road Dam section; Sample No. 42; 58.74 μm); l) *Glaphyrocysta semitecta* (Servez Road Dam section; Sample No. 42; 58.62 μm).

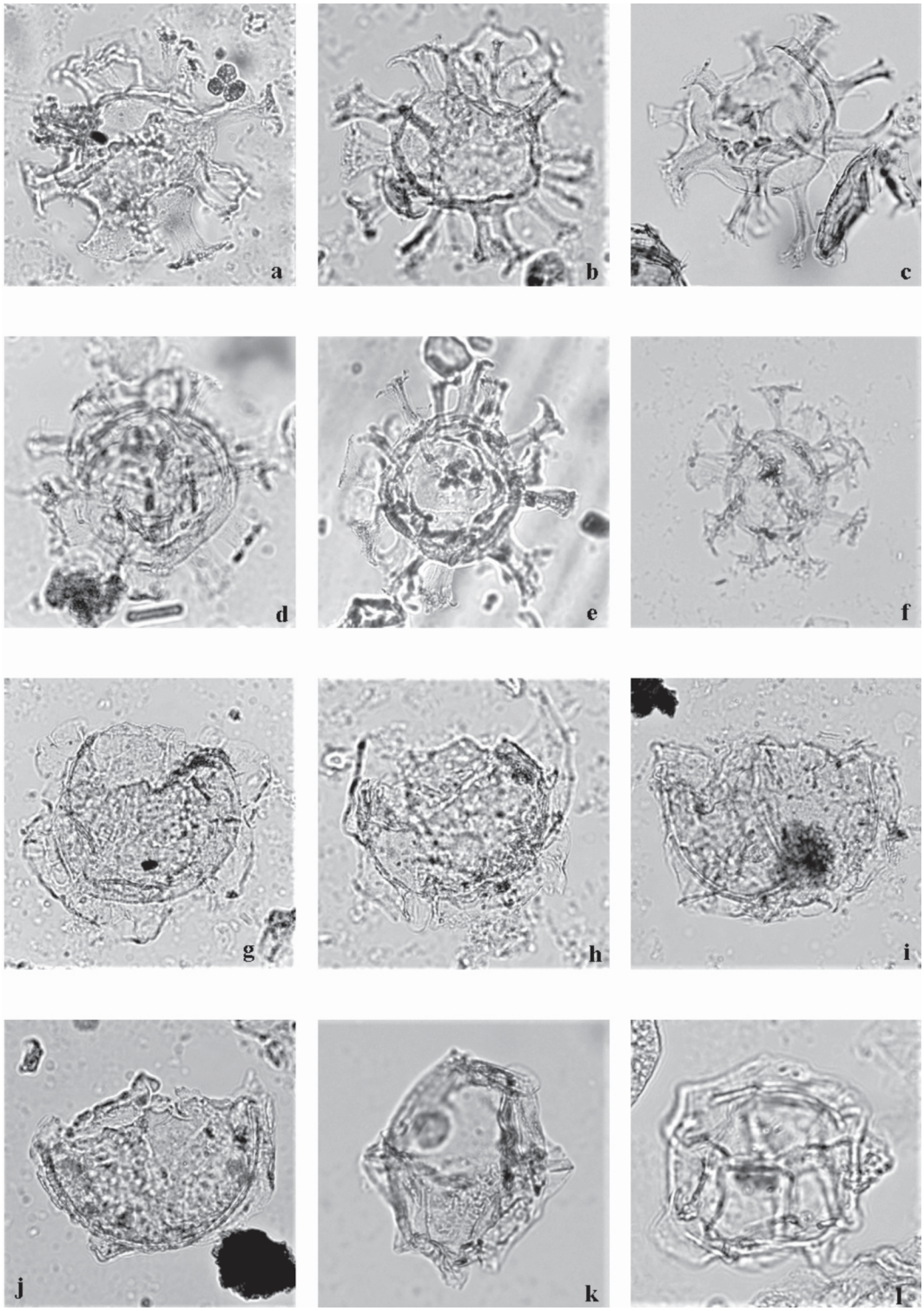

Figure 11. a) *Cordosphaeridium cantharellus* (Karaburun (1) section; Sample No. 171; 66.20 µm); b) *Cordosphaeridium cantharellus* (Sazlıbosna section; Sample No. 5; 60.68 µm); c) *Cordosphaeridium cantharellus* (Servez Road Dam section; Sample No. 42; 69.65 µm); d) *Cordosphaeridium cantharellus* (Servez Beach section; Sample No. 76; 47.58 µm); e) *Cordosphaeridium cantharellus* (Karaburun (1) section; Sample No. 171; 78.62 µm); f) *Cordosphaeridium minimum* (Servez Road Dam section; Sample No. 42; 28.27 µm); g) *Areoligera tauloma-sentosa* (Sazlıbosna section; Sample No. 5; 77.93 µm); h) *Areoligera tauloma-sentosa* (Sazlıbosna section; Sample No. 5; 77.48 µm); i) *Areoligera tauloma-sentosa* (Sazlıbosna section; Sample No. 5; 60.00 µm); j) *Membranophoridium* cf. *connectum* (Karaburun (1) section; Sample No. 172; 67.58 µm); k) *Pentadinium laticinctum* (Servez Road Dam section; Sample No. 42; 44.82 µm); l) *Pentadinium* sp. (Servez Beach section; Sample No. 76; 41.37 µm).

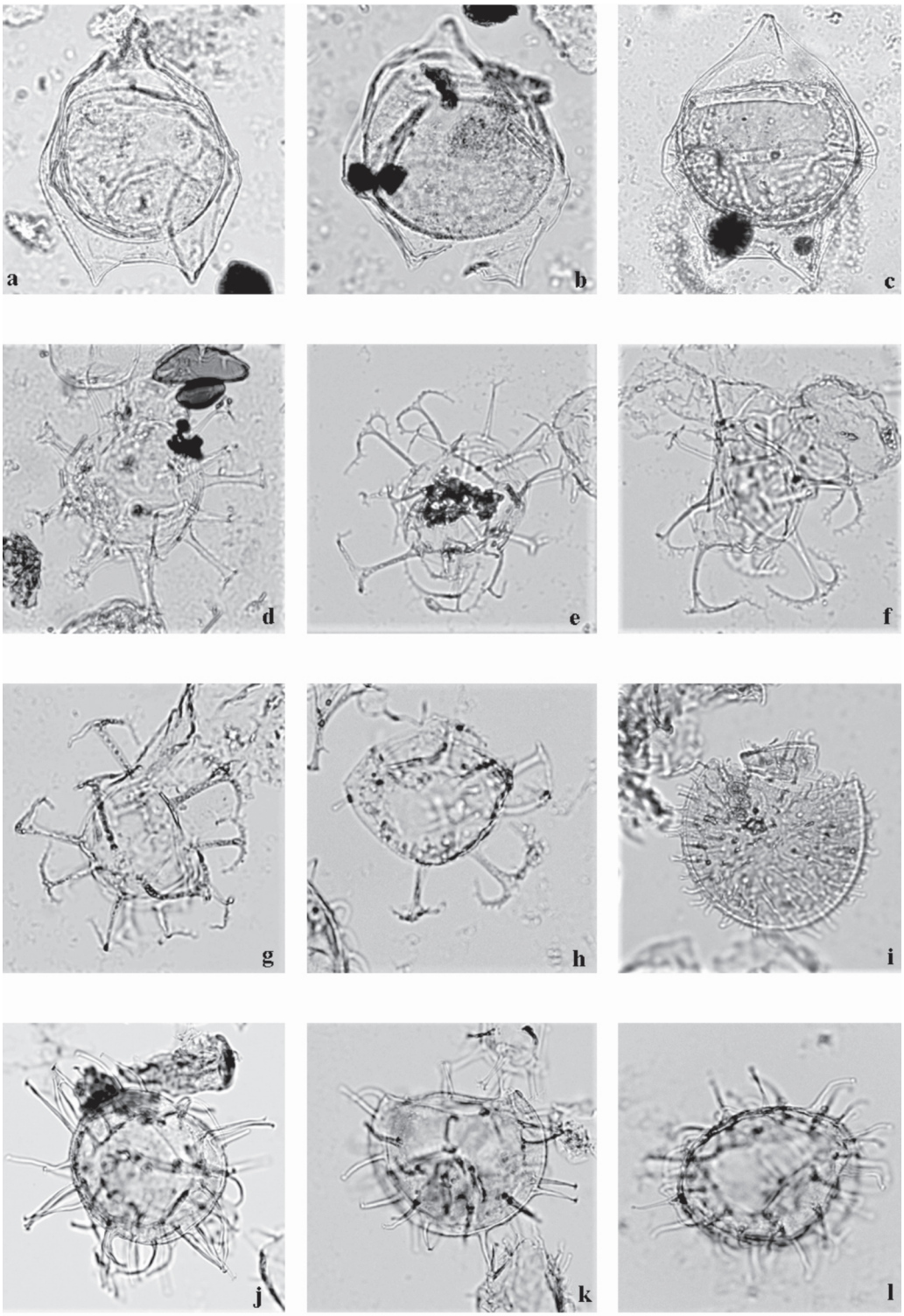

Figure 12. a) *Deflandrea phosphoritica* (Sazlıbosna section; Sample No. 5; 73.10 µm); b) *Deflandrea phosphoritica* (Sazlıbosna section; Sample No. 5; 67.58 µm); c) *Deflandrea* cf. *granulosa* (Karaburun (1) section; Sample No. 171; 88.27 µm); d) *Homotryblium tenuispinosum* (Servez Beach section; Sample No. 76; 48.27 µm); e) *Enneadocysta pectiniformis* (Servez Road Dam section; Sample No. 42; 44.82 µm); f) *Enneadocysta pectiniformis* (Servez Road Dam section; Sample No. 42; 42.75 µm); g) *Enneadocysta pectiniformis* (Servez Road Dam section; Sample No. 42; 44.64 µm); h) *Enneadocysta pectiniformis* (Servez Road Dam section; Sample No. 42; 34.48 µm); i) *Operculodinium* sp. (Servez Road Dam section; Sample No. 42; 45.51 µm); j) *Operculodinium* sp. (Servez Road Dam section; Sample No. 42; 98.62 µm); k) *Operculodinium* sp. (Servez Road Dam section; Sample No. 42; 63.44 µm); l) *Operculodinium* sp. (Servez Road Dam section; Sample No. 42; 54.48 µm).

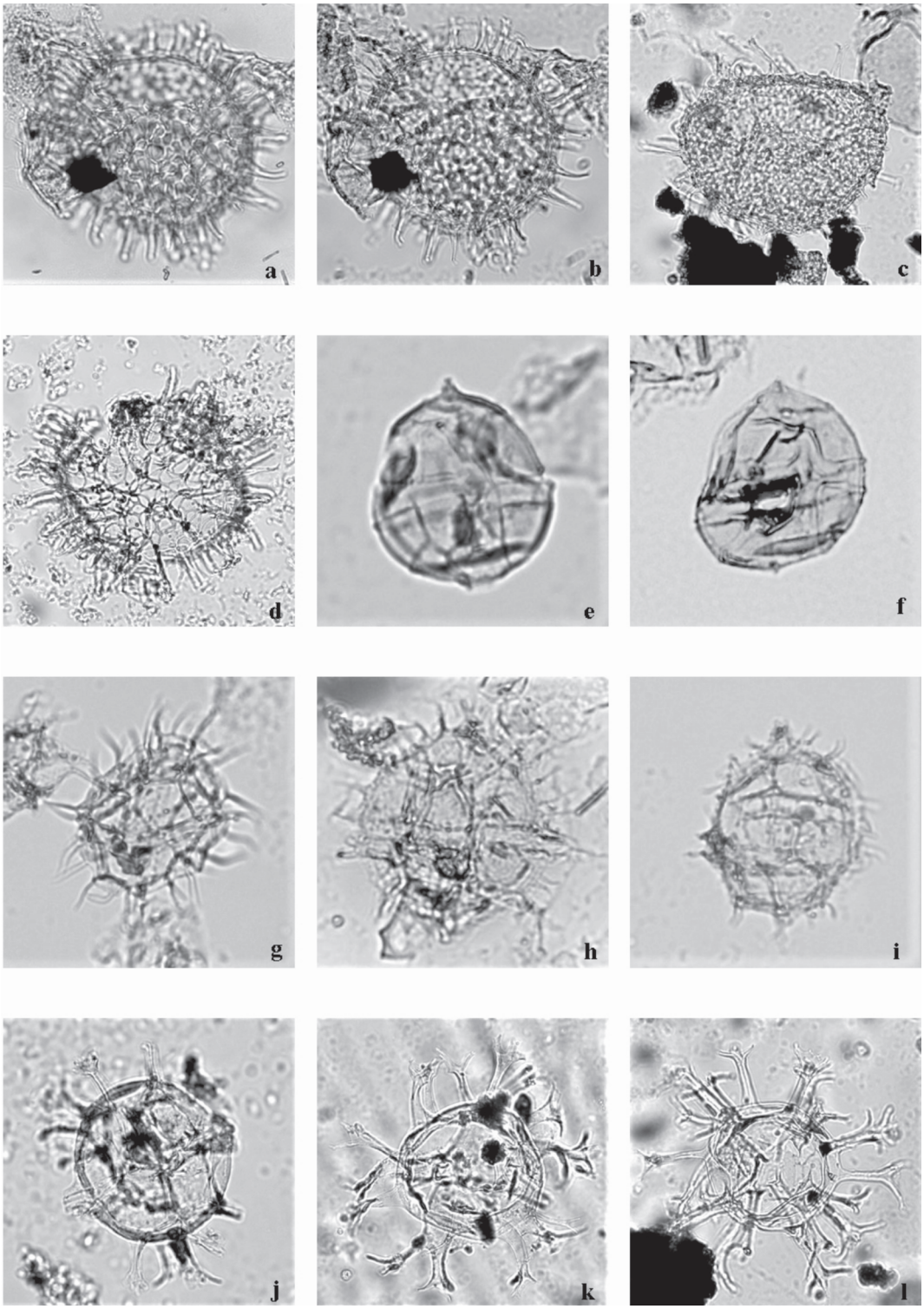

Figure 13. a) *Cordosphaeridium funiculatum* (High focus; Servez Beach section; Sample No. 76; 71.72 µm); b) *Cordosphaeridium funiculatum* (Low focus; Servez Beach section; Sample No. 76; 71.72 µm); c) *Cordosphaeridium funiculatum* (Karaburun (1) section; Sample No. 172; 73.10 µm); d) *Cordosphaeridium funiculatum* (Sazlıbosna section; Sample No. 4; 73.24 µm); e) *Phthanoperidinium amoenum* (Servez Road Dam section; Sample No. 42; 23.44 µm); f) *Phthanoperidinium amoenum* (Servez Road Dam section; Sample No. 42; 21.37 µm); g) *Phthanoperidinium comatum* (Servez Road Dam section; Sample No. 42; 31.03 µm); h) *Phthanoperidinium comatum* (Servez Beach section; Sample No. 76; 31.16 µm); i) *Phthanoperidinium comatum* (Servez Road Dam section; Sample No. 42; 24.13 µm); j) *Spiniferites pseudofurcatus* (Sazlıbosna section; Sample No. 5; 66.20 µm); k) *Achomosphaera alcicornu* (Karaburun (1) section; Sample No. 172; 88.96 µm); l) *Achomosphaera alcicornu* (Karaburun (1) section; Sample No. 172; 85.51 µm).

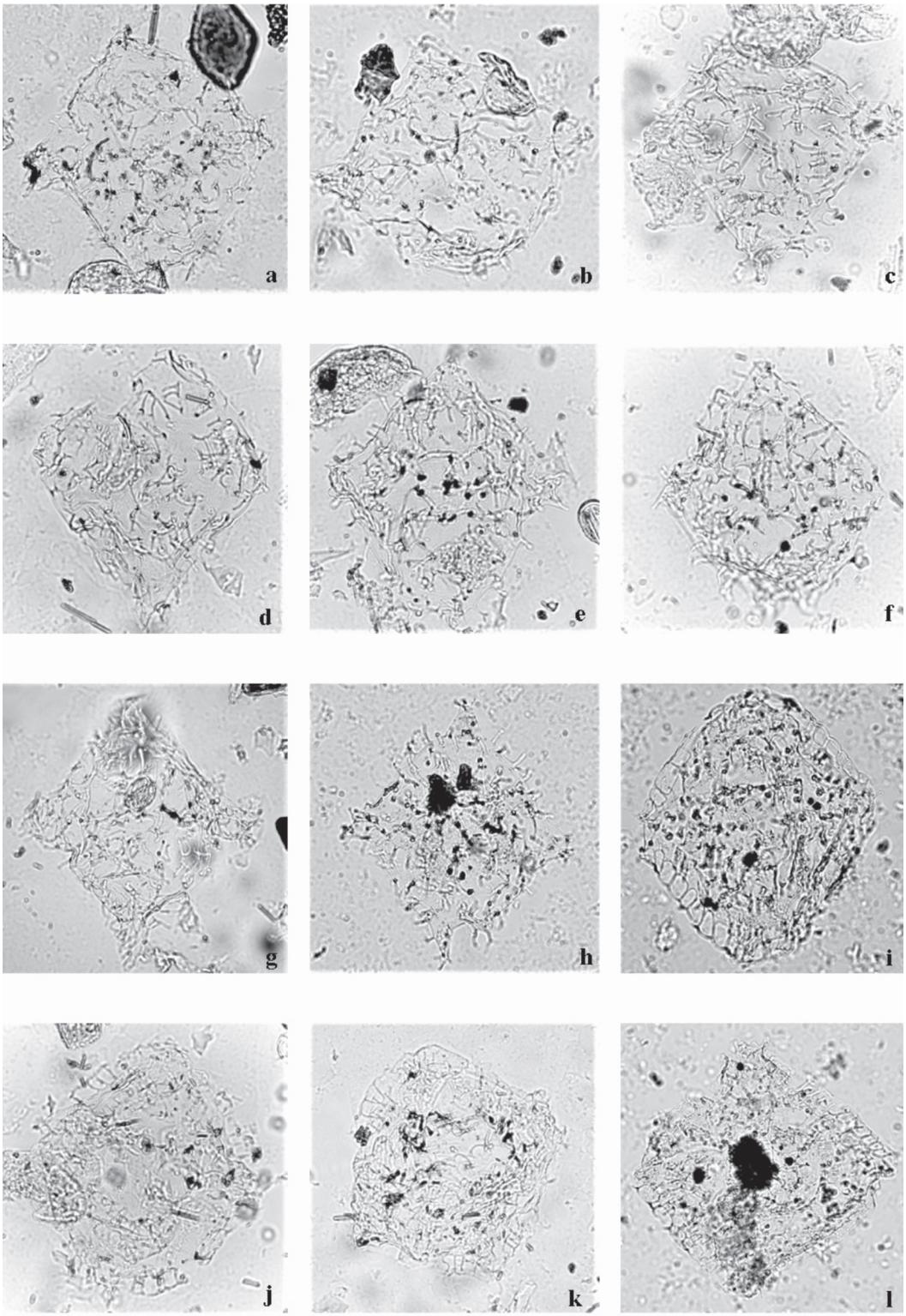

Figure 14. a) *Wetzeliella gochtii* (Servez Beach section; Sample No. 76; 46.89 µm); b) *Wetzeliella gochtii* (Servez Beach section; Sample No. 76; 72.41 µm); c) *Wetzeliella gochtii* (Servez Beach section; Sample No. 76; 82.75 µm); d) *Wetzeliella gochtii* (Servez Beach section; Sample No. 76; 63.44 µm); e) *Wetzeliella gochtii* (Servez Beach section; Sample No. 76; 70.34 µm); f) *Wetzeliella gochtii* (Servez Beach section; Sample No. 76; 66.20 µm); g) *Wetzeliella symmetrica* (Servez Beach section; Sample No. 76; 70.47 µm); h) *Wetzeliella symmetrica* (Karaburun (1) section; Sample No. 172; 68.27 µm); i) *Charlesdowniea clathrata* (Sazlıbosna section; Sample No. 5; 85.51 µm); j) *Charlesdowniea clathrata* (Servez Beach section; Sample No. 76; 48.27 µm); k) *Charlesdowniea clathrata* (Servez Beach section; Sample No. 76; 66.20 µm); l) *Charlesdowniea clathrata* (Sazlıbosna section; Sample No. 5; 89.65 µm).

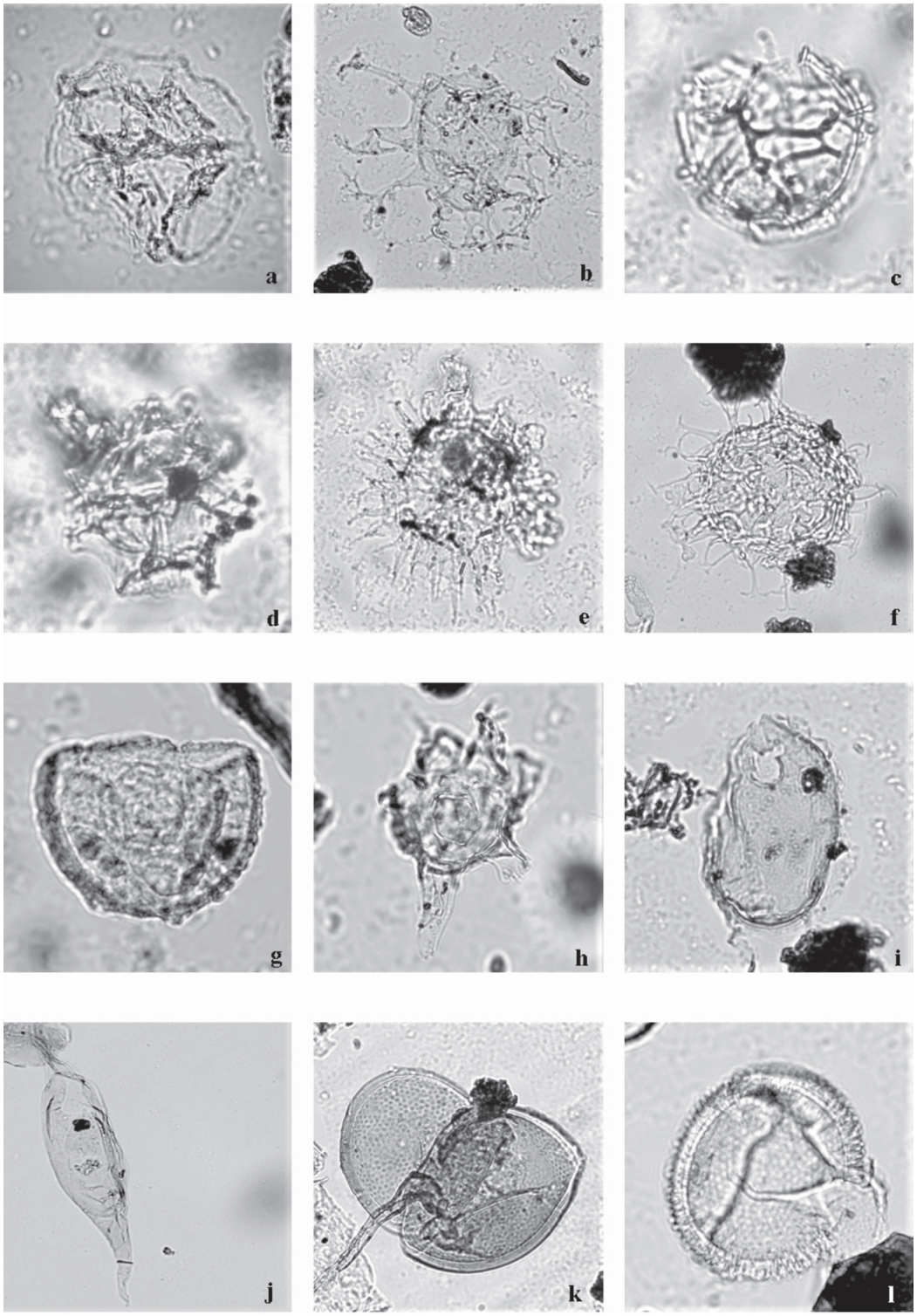

Figure 15. a) *Ascostomocystis potana* (Karaburun (1) section; Sample No. 172; 51.72 μm); b) *Distatodinium ellipticum* (Karaburun (1) section; Sample No. 172; 55.17 μm); c) *Impagidinium dispertitum* (Karaburun (1) section; Sample No. 171; 29.65 μm); d) *Impagidinium velorum* (Karaburun (1) section; Sample No. 171; 24.82 μm); e) *Lingulodinium machaerophorum* (Karaburun (1) section; Sample No. 171; 44.82 μm); f) *Cleistosphaeridium placacanthum* (Servez Road Dam section; Sample No. 38; 48.27 μm); g) *Stoveracysta ornata* (Sazlıbosna section; Sample No. 5; 35.86 μm); h) *Hystrichokolpoma* sp. (Karaburun (1) section; Sample No. 172; 52.41 μm); i) *Cyclopsiella lusatica* (Servez Beach section; Sample No. 73; 35.17 μm); j) *Palaeocystodinium* sp. (Servez Road Dam section; Sample No. 42; 86.20 μm); k) *Tasmanites* (Servez Beach section; Sample No. 73; 73.79 μm); l) *Tasmanites* (Servez Beach section; Sample No. 76; 37.93 μm).

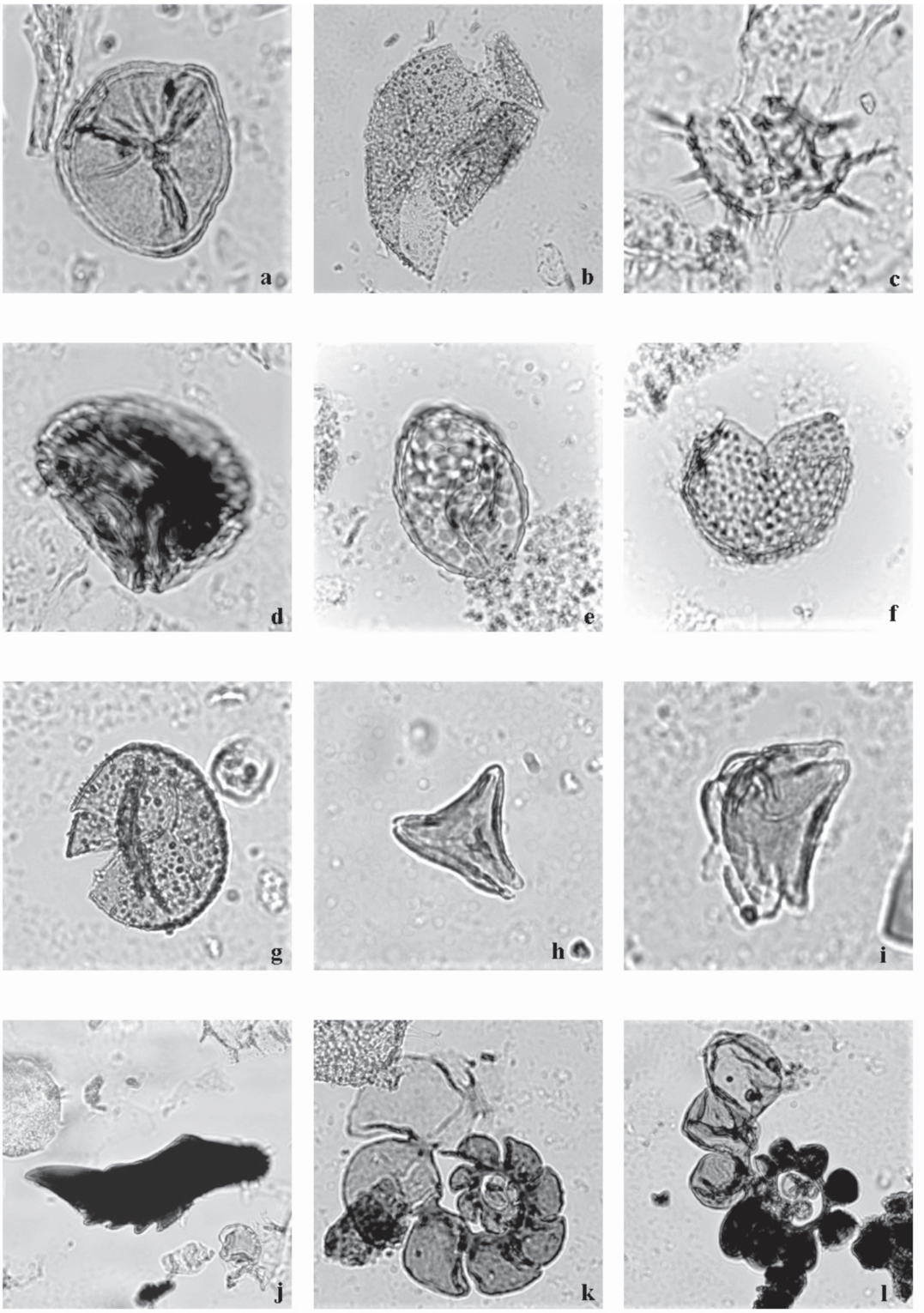

Figure 16. a) *Lusatisporites perinatus* (Servez Beach section; Sample No. 76; 27.58 µm); b) *Baculatisporites gemmatus* (Servez Beach section; Sample No. 76; 55.86 µm); c) *Echinatisporis* sp. (Servez Beach section; Sample No. 76; 26.89 µm); d) *Cicatricosisporites dorogensis* (Servez Beach section; Sample No. 76; 27.58 µm); e) *Verrucatosporites favus* (Sazlıbosna section; Sample No. 5; 31.03 µm); f) *Schizosporis* sp. (Sazlıbosna section; Sample No. 5; 24.82 µm); g) *Schizosporis* sp. (Servez Beach section; Sample No. 73; 36.55 µm); h) *Slowakipollis hippophaeoides* (Servez Beach section; Sample No. 73; 20.68 µm); i) *Slowakipollis hippophaeoides* (Servez Beach section; Sample No. 73; 21.37 µm); j) Scolecodont (Servez Beach section; Sample No. 76; 44.82 µm); k) Foraminiferal linings (Karaburun (1) section; Sample No. 172; 70.34 µm); l) Foraminiferal linings (Karaburun (1) section; Sample No. 172; 54.48 µm).

Eocene dinoflagellates such as *Areoligera tauloma-sentosa*, *Areosphaeridium michoudii*, *Rhombodinium perforatum*, *Homotryblium pallidum*, and *Stoveracysta ornata* and a lack of Oligocene taxa.

Hemiplacophora semilunifera is a stratigraphically important taxon. Even though this species was identified in the Late Eocene in Browns Creek Clays, SW Victoria, Australia (Cookson and Eisenack, 1965), its last occurrence defines the upper boundary of the Gse zone (Brinkhuis and Biffi, 1993; Brinkhuis, 1994; Wilpshaar et al., 1996; Torricelli and Biffi, 2001) within the early Rupelian (Figure 7). It was also reported in earliest Rupelian sediments in the Caspian Region (Batı, 2015). However, *H. semilunifera* was only identified in the Sazlıbosna section (Sample 5) in the late Priabonian interval in this study (Figure 8). As was mentioned in the previous section, this might be related to the absence of the latest Priabonian (top of Aal zone) and the earliest Rupelian (Gse zone) levels due to the unconformity and unfavourable lithologies of the Soğucak Formation. Furthermore, the distinction between the Gse and Adi zones is not clear since the continuous occurrence of *H. semilunifera* was not observed and the LO of *H. semilunifera* is only questionable in the studied sections.

5.2. Assemblage Zone B

Age Assignment: Earliest Rupelian

Corresponding dinoflagellate zone: Adi (*Areosphaeridium diktyoplokum*) and Rac (*Reticulatosphaera actinocoronata*) zones

Corresponding planktonic foraminiferal zone: P18

Corresponding nannoplankton zone: NP21

Corresponding Eastern Paratethyan Regional Stage: Pshekhian

Samples: Servez Road Dam (samples 35, 38, and 42)

This interval is characterized by the common occurrence of *Glaphyrocysta semitecta* and the LO of *A. diktyoplokum*.

The LO of *A. diktyoplokum* at 33.3 Ma, in the earliest Rupelian, was reported by Williams et al. (2004) in their comprehensive study of magnetostratigraphically calibrated first and last occurrences of selected dinoflagellate cysts in the mid-latitudes of the northern hemisphere. The earliest Rupelian LO of *A. diktyoplokum* at 33.3 Ma was also confirmed by Pross et al. (2010) in an Oligocene succession of Italy where this event was documented within the uppermost Chron C13n at 33.3 Ma in the earliest Oligocene (NP21), at the boundary of the Adi–Rac zones based on magnetostratigraphic calibration. This dinoflagellate cyst event was recorded slightly earlier at 33.6–33.4 Ma in the earliest Oligocene (NP21 and at the P17–18 boundary) at higher latitudes in the Norwegian-Greenland Sea (Eldrett et al., 2004). The LO of *A. diktyoplokum* was identified in the Gse and Adi zones and consistently in the earliest Oligocene in Italy (Brinkhuis and Biffi, 1993; Brinkhuis, 1994). Just above the LO of *A. diktyoplokum*, the FO of *W. gochtii* was recorded in the Rac zone in the earliest Early Oligocene in their study. Similar stratigraphical distributions of those taxa were also recorded in the earliest Oligocene successions in the Western Black Sea in the same stratigraphical order as in this present study (Figure 8).

The LO of *G. semitecta* is an important zonal marker dinoflagellate cyst event and was recorded in the lower part of Chron C12r at 32.5 Ma in the Central Mediterranean (Wilpshaar et al., 1996) and in the lower part of Chron C12r at 32.6 Ma (in NP22) at the boundary of the Rac–Cin zones in the Western Tethys (Pross et al., 2010). This taxon seems to have a near-synchronous LO at 32.0 Ma in the northern hemisphere's mid-latitudes (Williams et al., 2004) and in the higher latitudes where it was also reported in the middle of NP22 in the North Sea (Van Simaeys et al., 2005).

The presence of a hiatus between the Eocene and Oligocene units was confirmed by the lack of the earliest Rupelian dinoflagellate biozone (Gse zone of Brinkhuis and Biffi, 1993; Brinkhuis, 1994; Wilpshaar et al., 1996; Torricelli and Biffi, 2001) in this study (Figures 7 and 8). The Gse zone (earliest Rupelian), defined by the interval between the FO of *G. semitecta* and the LO of *Hemiplacophora semilunifera*, is missing in the studied sections (except perhaps at Servez Beach, where unsuitable lithologies dominate this interval) and confirms the unconformable nature of Eocene-Oligocene boundary in the studied area.

5.3. Assemblage Zone C

Age Assignment: Early Rupelian

Corresponding dinoflagellate zones: Rac (*Reticulatosphaera actinocoronata*), Cin (*Corrudinium incompositum*), and Hpu (*Hystrichokoplpoma pusillum*) zones

Corresponding planktonic foraminiferal zone: P18–19

Corresponding nannoplankton zone: NP22–23

Corresponding Eastern Paratethyan Regional Stage: Pshekhian

Samples: Karaburun (1) (samples 171 and 172) and the lower part of Servez Beach (samples 75 and 76)

This interval is distinguished by *Wetzeliella gochtii*-bearing samples. *Melitasphaeridium choanophorum* also occurs for the first time in this interval.

The stratigraphical importance of the LO of *Areosphaeridium diktyoplokum* and the FO of *W. gochtii* has been known and used from a biostratigraphical point of view for decades (e.g., Liengjarern et al., 1980; Brinkhuis, 1992, 1994; Powell, 1992; Brinkhuis and Biffi, 1993; Bujak and Mudge, 1994; Toricelli and Biffi, 2001; Williams et al., 2004). However, as was explained in detail by Pross (2001), the FO and LO of wetzelielloid

dinoflagellate cysts including *W. gochtii* reflect strong diachronism in that 3.6 Myr of time difference might have occurred in different regions of Europe. The oldest FO of *W. gochtii* was reported from the Polish Carpathians in the Late Eocene (van Couvering et al., 1981; Gedl, 2004a). However, in addition to several studies pointing out the Rupelian FO of *W. gochtii* (e.g., Brinkhuis, 1992, 1994; Powell, 1992; Brinkhuis and Biffi, 1993; Toricelli and Biffi, 2001; Köthe and Piesker, 2007; Soliman, 2012), an early Rupelian FO of *W. gochtii* was also highlighted in several magnetostratigraphically calibrated dinocyst studies. Williams et al. (2004) documented this event at 32.8 Ma in the early Rupelian. Similarly, the FO of *W. gochtii* was encountered in the lower part of Chron C12r at 33.1 Ma in the early Rupelian (at the NP21–22 boundary) within the Rac zone based on magnetostratigraphical calibration in Italy (Pross et al., 2010), whereas it has a slightly older FO at 33.6–33.2 Ma but still within the early Rupelian (close to the NP21–22 boundary) at higher latitudes in the Norwegian-Greenland Sea (Eldrett et al., 2004) and at the base of NP22 in the southern North Sea basin (Van Simaeys et al., 2005). The same event was also reported from slightly younger sediments in NP23 in the Northern Caucasus (Zaporozhets, 1999; Sachsenhofer et al., 2017). A similar stratigraphic distribution of this taxon occurs in the P-Rp2 zone in Eastern Anatolia (Sancay, 2005; Batı and Sancay, 2007), corresponding to the Hpu zone, NP23, and the *Wetzeliella gochtii-Distatodinium ellipticum* zone in NP23–24 in Thrace (Bati et al., 1993, 2007).

Recently, Gürgey and Batı (2018) subdivided the Lower Oligocene Mezardere Formation in the Thrace Basin informally into the Lower Mezardere Formation (LMF) and Upper Mezardere Formation (UMF) and distinguished two dinocyst assemblages in the Rupelian (Pshekhian to Solenovian). Even though long-ranging cosmopolitan dinoflagellates such as *Homotryblium* spp., *Cordosphaeridium* spp., *Distatodinium* spp., *Operculodinium* spp., *Cleistosphaeridium* spp., and *Spiniferites* spp. dominate both of the assemblages, some age-diagnostic taxa were also encountered. The lower part of the studied interval (LMF) has *Glaphyrocysta* cf. *semitecta* and was interpreted as ?Pshekhian (NP21/22) in age, whereas the *W. gochtii*-bearing upper part (UMF) was reported as Solenovian (NP23–24), based on the FO and LO of *W. gochtii*. The LO of *G. semitecta* is in the Rac zone, NP21. Therefore, the LMF of Gürgey and Batı (2018) might correspond to the Gse-Adi-Rac zones in the early Pshekhian (earliest Rupelian), based on the presence of *G. semitecta*. Additionally, a Solenovian (late Rupelian) age was assigned for the overlying UMF based on the early Chattian LO of *W. gochtii* in the same study. The lack of other zonal marker dinocysts for the Rupelian, such as *A. diktyoplokum*, *H. pusillum*, *Homotryblium oceanicum*, *Chiropteridium lobospinosum*, and *Distatodinium biffii*, coupled with the absence of *Chiropteridium* and *Deflandrea* acmes and the diachronous nature of the LO of *W. gochtii*, made a Solenovian age questionable for the UMF. Even so, some additional evidence for Solenovian strata exist in the Thrace Basin, such as high fresh-water influx (seen as *Pediastrum* blooms accompanied by common terrestrial palynomorphs) and the presence of manganese ore deposits (Gürgey and Batı, 2018). Brackish water conditions in the Thrace Basin and in many other localities of the Eastern Paratethys (Schulz et al., 2004, 2005; İslamoğlu et al., 2008; Bechtel et al., 2012; Batı, 2015; Gürgey and Batı, 2018 and references therein; Popov et al., 2019) were well known in the late Solenovian (late Rupelian). These unfavourable brackish depositional conditions might have resulted in reduced diversity of dinoflagellates, and cosmopolitan dinoflagellate taxa might have become dominant during the Solenovian in the Thrace Basin.

The youngest occurrence of *Charlesdowniea clathrata* has been identified at 102 m in the Ceylan Formation at the Servez Beach section in this study and confirms the early Rupelian interpretation. The LO of *C. clathrata* was magnetostratigraphically calibrated as 32.3 Ma in the middle part of Chron C12r in the early Rupelian in the Cin zone (Pross et al., 2010). Additionally, the FO of *Oligokolpoma galeottii* was also encountered at 96 m (sample 75 in Figure 4) at Servez Beach in this study (Figure 8). The FO of this taxa was magnetostratigraphically calibrated at 32.2 Ma in the Hpu zone in NP23 in Italy (Pross et al., 2010).

Sample 172 in the Karaburun (1) section was also studied micropalaeontologically (Shikhlinsky and Batı, 2008) and an Early Oligocene foraminifera assemblage was recorded: *Globorotalia* aff. *opima opima*, *Globigerina officinalis marna*, *Globigerina ampliapertura*, *G. pseudovenezuelana*, *Cassigerinella chipolensis*, *Uvigerina longa*, *Caucasina* cf. *tenebricoda*, *Elphidium minitum*, *Nonion* aff. *dozularensis*, *N. maragensis*, *Florilus boueanus*, *Cibicides sigmodialis*, *C. pseudoungerianus*, C. *tenellus*, and *C. borislavebsis*.

5.4. Assemblage Zone D

Age Assignment: Early-middle Rupelian

Corresponding dinoflagellate zones: Cin (*Corrudinium incompositum*) and Hpu (*Hystrichokoplpoma pusillum*) zones

Corresponding planktonic foraminiferal zone: P18–19

Corresponding nannoplankton zone: NP22–23

Corresponding Eastern Paratethyan Regional Stage: Pshekhian

Samples: The highest sample of Karaburun (2) (sample 176) and the upper part of Servez Beach (samples 72 and 73)

Samples belonging to this interval are recognized above the *Wetzeliella gochtii*-bearing intervals and yielded *Achomosphaera alcicornu*, *Enneadocysta pectiniformis*, *Membranophoridium aspinatum*, *Cordosphaeridium funiculatum*, *Areoligera semicirculata*,

Ascostomocystis potana, *Oligokolpoma galeottii*, and *Cordosphaeridium cantharellus* with common occurrences of *Cleistosphaeridium placacanthum*.

The presence of *E. pectiniformis* in the uppermost sample (sample 176 of Karaburun (2)) of the studied sections is stratigraphically important because the LO of this taxon in the northern hemisphere's mid-latitudes occurred at 29.3 Ma, within the Rupelian (Williams et al., 2004), based on magnetostratigraphical calibration. The LO of *E. pectiniformis* was reported in the "middle" Rupelian in Germany (Köthe and Piesker, 2007) and in the North Sea (van Simaeys et al., 2004, 2005). The last common occurrence of the same taxon was determined in the Cin zone, in the late Rupelian in Italy (Brinkhuis and Biffi, 1993; Brinkhuis, 1994).

Servez Beach (samples 72 and 73) was also studied micropalaeontologically and an Early Oligocene age was assigned based on the presence of *Globigerina tapuriensis*, *G. pseudoampliapertura*, *G. ouachitaensis*, *G. ampliapertura*, *Pseudohastigerina barbadoensis*, *Uvigerina costellata*, *U. oligocaenica*, *Gyroidina soldanii*, *Pseudoparella caucasica*, *Rotalia binaensis*, *Chilostomella normalis*, *Cibicides amphisyliensis*, and *Bolivina nolata oligocaenica* (Shikhlinsky and Batı, 2008).

6. Notes on depositional environment

Palaeoecological preferences of dinoflagellates (particularly in recent taxa) are very good criteria for palaeoenvironmental reconstructions (e.g., Brinkhuis and Biffi, 1993; Brinkhuis, 1994; Stover et al., 1996; Pross and Schmiedl, 2002; Gedl, 2005; Pross and Brinkhuis, 2005). As far as the dinoflagellate assemblages of the Western Black Sea region are concerned, the common occurrences (up to 14.48%) of *Homotryblium* spp. in all of the studied sections in the late Priabonian to early Rupelian suggest shallow-marine, inner neritic, and highly productivity conditions. Nutrient-rich and shallow-marine conditions were also confirmed by the presence of peridinioids such as *Deflandrea* and *Wetzeliella*. Several dinoflagellate taxa having shallow-marine, near-shore preferences such as *Areoligera*, *Glaphyrocysta*, *Polysphaeridium*, *Areosphaeridium*, and *Lingulodinium* were commonly observed in the studied sections. The rare occurrences (1.02% to 2.04%) of oceanic taxa of *Impagidinium* in the late Priabonian-early Rupelian and the presence of *Thalassiphora pelagica*, *Hystrichokolpoma*, and *Palaeocystodinium* in the early Rupelian may suggest that open-marine conditions prevailed sporadically. The presence of *Wetzeliella* and *Impagidinium* in the same samples of the Karaburun (1) section might have occurred due to stratified nutrient availability, in that the lower part of the water column had higher nutrient content than oligotrophic surface waters (Gedl, 2004b).

After the major sea-level fall at the Eocene/Oligocene boundary in the Eastern Paratethys, including the Thrace and Western Black Sea regions (Popov et al., 2010), a long-term transgression prevailed during the Early Oligocene (Turgut and Eseller, 2000; Gürgey and Batı, 2018). In the Thrace Basin, shallower brackish, neritic conditions in the early Rupelian (?Pshekhian) were replaced by brackish, dinocyst-rich, neritic, and nutrient-rich environments in the middle-late Rupelian (Solenovian) (Gürgey and Batı, 2018). No indications of fresh-water influx or brackish depositional settings were recorded during the late Priabonian-early Rupelian in the studied sections corresponding to NP21–23 in the Western Black Sea, where much more diverse and abundant marine palynomorphs were encountered, indicating mainly shallow-marine to open-marine, neritic, and nutrient-rich depositional conditions. Thus, even though the Western Black Sea and Thrace Basin were considered as part of the Paratethys during the Rupelian, palaeoenvironmental interpretations might be further evaluated as the studied sections (representing NP21–23) in the current study were deposited before the isolation of the Paratethys, when the Western Black Sea region was still part of the Western Tethys during the earliest Oligocene.

7. Conclusions

Four biochronostratigraphic intervals were identified based on marine palynomorphs in Upper Eocene to Lower Oligocene sediments in this study. The late Priabonian, below the *Glaphyrocysta semitecta* zone, is represented by the presence of Eocene species such as *Areoligera tauloma-sentosa*, *Areosphaeridium michoudii*, *Rhombodinium perforatum*, *Homotryblium pallidum*, and *Stoveracysta ornata*. The earliest Rupelian interval below the *Wetzeliella gochtii*-bearing samples is characterized by common occurrences of *G. semitecta* and the LO of *Areosphaeridium diktyoplokum*. The early Rupelian interval may be recognized by the presence of *W. gochtii* and the FO of *Melitasphaeridium choanophorum*. The early-middle Rupelian interval is represented by samples overlying the *W. gochtii*-bearing sediments and by the presence of *Achomosphaera alcicornu*, *Enneadocysta pectiniformis*, *Membranophoridium aspinatum*, *Cordosphaeridium funiculatum*, *Areoligera semicirculata*, *Ascostomocystis potana*, *Oligokolpoma galeottii*, and *Cordosphaeridium cantharellus* and common occurrences of *Cleistosphaeridium placacanthum*.

Palynomorph and organic matter assemblages clearly indicate shallow- to open-marine and nutrient-rich depositional conditions for the deposition of Upper Eocene to Lower Oligocene sediments in the study area. The studied sections are dominated by marine palynomorphs without any indication of fresh-water influx and might represent deposition before the isolation of the Paratethys,

when the Western Black Sea region was still part of the Western Tethys during the earliest Oligocene (NP21–23).

Based on the palynological biozonations, the nature of the Eocene-Oligocene boundary can be classified as an unconformity at the Karaburun and Sazlıbosna localities, whereas it seems to be transitional at Servez Beach.

Acknowledgements
We are grateful to Turkish Petroleum Corporation for giving permission for this paper to be published. We appreciate Keith Richards for his constructive and helpful comments on the manuscript. We would like to thank Muzaffer Siyako and Doğan Alaygut for their contributions during the field study. We also thank Mine Sezgül Kayseri for her technical support in drawings. Special thanks go to Aral I Okay, Ercan Özcan, and Gabor Tari for their comments and suggestions about the study area. Finally, we would like to express our sincere thanks to the anonymous reviewers for their valuable comments and contributions to the text.

References

Alegret L, Cruz LE, Fenero R, Molina E, Ortiz S et al. (2008). Effects of the Oligocene climatic events on the foraminiferal record from Fuente Caldera section (Spain, Western Tethys). Palaeogeography, Palaeoclimatology, Palaeoecology 269: 94-102.

Batı Z (2015). Dinoflagellate cyst biostratigraphy of the upper Eocene and lower Oligocene of the Kirmizitepe Section, Azerbaijan, South Caspian Basin. Review of Palaeobotany and Palynology 217: 9-38.

Batı Z, Erk S, Akça N (1993). Trakya Havzası Tersiyer birimlerinin palinomorf, foraminifer ve nannoplankton biyostratigrafisi. TPAO Rep No: 1947. Ankara, Turkey: TPAO (in Turkish).

Batı Z, Pinçe S, Akça N (2007). Biostratigraphical properties of the Priabonian-Rupelian (Upper Eocene-Lower Oligocene) boundary in the Thrace Basin. In: Abstracts of Turkish Stratigraphy Committee Workshop. Ankara, Turkey: MTA, p. 14.

Batı Z, Sancay RH (2007). Palynostratigraphy of Rupelian sediments in the Muş Basin, Eastern Anatolia, Turkey. Micropaleontology 53: 249-283.

Bechtel A, Hamor-Vido M, Gratzer R, Sachsenhofer RF, Pütmann W (2012). Facies evolution and stratigraphic correlation in the early Oligocene Tard Clay of Hungary as revealed by maceral, biomarker and stable isotope composition. Marine and Petroleum Geology 35: 55-74.

Berggren WA, Kent DV, Swisher CC 3rd, Aubry MP (1995). A revised Cenozoic geochronology and chronostratigraphy. SEPM Special Publications 54: 129-212.

Bodiselitsch B, Montanari A, Koeberl C, Coccioni R (2004). Delayed climate cooling in the Late Eocene caused by multiple impacts: High-resolution geochemical studies at Massignano, Italy. Earth and Planetary Sciences Letters 223: 283-302.

Brinkhuis H (1992). Late Eocene to Early Oligocene dinoflagellate cysts from central and northeast Italy. PhD, University of Utrecht, Utrecht, the Netherlands.

Brinkhuis H (1994). Late Eocene to Early Oligocene dinoflagellate cysts from the Priabonian type-area (Northeast Italy): biostratigraphy and paleoenvironmental interpretation. Palaeogeography, Palaeoclimatology, Palaeoecology 107: 121-163.

Brinkhuis H, Biffi U (1993). Dinoflagellate cyst stratigraphy of the Eocene/Oligocene transition in central Italy. Marine Micropaleontology 22: 131-183.

Bujak J (1994). New dinocyst taxa from the Eocene of the North Sea. Journal of Micropaleontology 13: 119-131.

Bujak J, Mudge D (1994). A high-resolution North Sea Eocene dinocyst zonation. Journal of the Geological Society of London 151: 449-462.

Coccioni R, Basso D, Brinkhuis H, Galeotti S, Gardin S et al. (2000). Marine biotic signals across a late Eocene impact layer at Massignano, Italy: evidence for long-term environmental perturbations? Terra Nova 12: 258-263.

Cookson IC, Eisenack A (1965). Microplankton from the Browns Creek Clays, SW. Victoria. Proceedings of the Royal Society of Victoria 79: 119-131.

Costa LI, Downie C, Eaton G (1976). Palynostratigraphy of some Middle Eocene sections from the Hampshire Basin (England). Proceedings of the Geologists' Association of London 87: 273-284.

Diester-Haass L, Zahn R (2001). Paleoproductivity increase at the Eocene–Oligocene climatic transition: ODP/DSDP sites 763 and 592. Palaeogeography, Palaeoclimatology, Palaeoecology 172: 153-170.

El Beialy SY, Head MJ, El Atfy H, El Khoriby EM (2019). Dinoflagellate cyst evidence for the age and palaeoenvironments of the Upper Eocene-Oligocene Dabaa Formation, Qattara Depression, north Western Desert, Egypt. Palynology 43: 268-291.

Eldrett J, Harding IC, Firth JV, Roberts AP (2004). Magnetostratigraphic calibration of Eocene-Oligocene dinoflagellate cyst biostratigraphy from the Norwegian–Greenland Sea. Marine Geology 204: 91-127.

Gedik İ, Timur E, Umut M, Bilgin AZ, Pehlivan Ş et al. (2014). Geological Maps of Turkey, 1: 50 000 scale İstanbul F21-A sheet and explanatory notes. Ankara, Turkey: MTA Genel Müdürlüğü.

Gedl P (2004a). Dinoflagellate cyst record of the Eocene-Oligocene boundary succession in flysch deposits at Leluchow, Carpathian Mountains, Poland. Geological Society of London Special Publications 230: 309-324.

Gedl P (2004b). Dinoflagellate cyst from the Sambron beds (Central Carpathian Paleogene) in Slovak Orava. Studia Geologica Polonica 123: 223-243.

Gedl P (2005). Late Eocene-Early Oligocene organic-walled dinoflagellate cysts from Folusz, Magura Nappe, Polish Carpathians. Acta Palaeobotanica 45: 27-83.

Görür N, Okay AI (1996). Fore-arc origin of the Thrace basin, northwest Turkey. Geologische Rundschau 85: 662-668.

Gültekin AH (1998). Geochemistry and origin of the Oligocene Binkılıç Manganese deposits, Thrace basin, Turkey. Turkish Journal of Earth Sciences 7: 11-24.

Gürgey K (2007). Geochemical characteristic and thermal maturity of oils from the Thrace Basin (western Turkey) and western Turkmenistan. Journal of Petroleum Geology 22: 167-189.

Gürgey K, Batı Z (2018). Palynological and petroleum geochemical assessment of the Lower Oligocene Mezardere Formation, Thrace Basin, NW Turkey, Turkish Journal of Earth Sciences 27: 349-383.

Head MJ, Norris G (1989). Palynology and dinocyst stratigraphy of the Eocene and Oligocene in ODP Leg 105, Hole 647A, Labrador Sea. Proceedings of the Ocean Drilling Program Scientific Results 105: 515-550.

Heilmann-Clausen C, van Simaeys S (2005). Dinoflagellate cysts from the Middle Eocene to ?lowermost Oligocene succession in the Kysing research borehole, Central Danish Basin. Palynology 29: 143-204.

Houben AJP, van Mourik CA, Montanari A, Brinkhuis H (2012). The Eocene–Oligocene transition: changes in sea level, temperature or both? Palaeogeography, Palaeoclimatology, Palaeoecology 335: 75-83.

İslamoğlu Y, Harzhauser M, Gross M, Jimenez-Moren G, Coric S et al. (2008). From Tethys to Eastern Paratethys: Oligocene depositional environments, paleoecology and paleobiogeography of the Thrace Basin (NW Turkey). International Journal of Earth Sciences 99: 183-200.

Kostopoulou S, Maravelis AG, Zelilidis A (2018). Biostratigraphic analysis across the Eocene–Oligocene boundary in the southern Hellenic Thrace basin (Lemnos Island, north Aegean Sea). Turkish Journal of Earth Sciences 27: 232-248.

Köthe A, Piesker B (2007). Stratigraphic distribution of Paleogene and Miocene dinocysts in Germany. Revue de Paleobiologie Genève 26: 1-39.

Less G, Özcan E, Okay AI (2011). Stratigraphy and larger foraminifera of the Middle Eocene to Lower Oligocene shallow-marine units in the northern and eastern parts of the Thrace Basin, NW Turkey. Turkish Journal of Earth Sciences 20: 793-845.

Liengjarern M, Costa LI, Downie C (1980). Dinoflagellate cysts from the Upper Eocene-Lower Oligocene of the Isle of Wight. Palaeontology 23: 475-499.

Mahboub I, Slimani H, Toufiq A, Chekar M, Djeya KL et al. (2019). Middle Eocene to early Oligocene dinoflagellate cyst biostratigraphy and paleoenvironmental interpretations of the Ben Attaya section at Taza, eastern External Rif, Morocco. Journal of African Earth Sciences 149: 154-169.

Medus J, Pairis JL (1990). Reworked pollen assemblages and the Eocene-Oligocene boundary in the Paleogene of the western external French Alps. Palaeogeography, Palaeoclimatology, Palaeoecology 81: 59-78.

Miller KG, Browning JV, Aubry MP, Wade BS, Katz ME et al. (2008). Eocene–Oligocene global climate and sea-level changes: St. Stephens Quarry, Alabama. Geological Society of America Bulletin 120: 34-53.

Miller KG, Wright JD, Fairbanks RG (1991). Unlocking the ice house: Oligocene-Miocene oxygen isotopes, eustasy, and margin erosion. Journal of Geophysical Research Atmospheres 96: 6829-6848.

Miller KG, Wright JD, Katz ME, Wade BS, Browning JV et al. (2009). Climate threshold at the Eocene-oligocene transition: Antarctic ice sheet influence on ocean circulation. In: Koeberl C, Mantanari A (editors). The Late Eocene Earth-Hothouse-Icehouse and Impacts. Boulder, CO, USA: Geological Society of America, pp. 169-178.

Natalin B, Say AG (2015). Eocene–Oligocene stratigraphy and structural history of the Karaburun area, southwestern Black Sea coast, Turkey: transition from extension to compression. Geological Magazine 152: 1104-1122.

Nikishin AM, Okay AI, Tüysüz O, Demirer A, Amelin N et al. (2015). The Black Sea basins structure and history: New model based on new deep penetration regional seismic data. Part 1: Basins structure and fill. Marine and Petroleum Geology 59: 638-655.

Okay AI (2016). The Eocene-Oligocene of the Karaburun-Çatalca Area, İstanbul, Field Guide. İstanbul, Turkey: Eurasia Institute of Earth Sciences and Department of Geology, Faculty of Mines, İstanbul Technical University.

Okay AI, Özcan E, Hakyemez A, Siyako M, Sunal G et al. (2019). The Thrace Basin and the Black Sea: the Eocene-Oligocene marine connection. Geological Magazine 156: 39-61.

Okay AI, Simmons M, Özcan E, Starkie S, Bidgood M (2020). Eocene-Oligocene succession at Kıyıköy (Midye) on the Black Sea coast in Thrace. Turkish Journal of Earth Sciences 29: 139-153.

Okay AI, Tansel İ, Tüysüz O (2001). Obduction, subduction and collision as reflected in the Upper Cretaceous-Lower Eocene sedimentary record of western Turkey. Geological Magazine 138: 117-142.

Okay AI, Tüysüz (1999). Tethyan sutures of northern Turkey. Geological Society of London Special Publications 156: 475-515.

Oktay FY, Eren RH, Sakınç M (1992). Sedimentary geology of the eastern Thrace Oligocene basin in the region of Karaburun-Yeniköy (Istanbul). In: Proceedings of the 9th Petroleum Congress of Turkey, Ankara, Turkey, pp. 92-101 (in Turkish with an abstract in English).

Özcan E, Okay AI, Bürkan KA, Yücel AO, Özcan Z (2018). Middle-Late Eocene marine record of the Biga Peninsula, NW Anatolia Turkey. Geologica Acta 16: 163-187.

Özcan Z, Okay AI, Özcan E, Hakyemez A, Özkan-Altiner S (2012). Late Cretaceous-Eocene geological evolution of the Pontides based on new stratigraphic and palaeontologic data between the Black Sea coast and Bursa (NW Turkey). Turkish Journal of Earth Sciences 21: 933-960.

Öztürk H, Frakes AL (1995). Sedimentation and diagenesis of an Oligocene manganese deposit in a shallow subbasin of the Paratethys: Thrace Basin, Turkey. Ore Geology Reviews 10: 117-132.

Pagani M, Zachos J, Freeman KH, Bohaty S, Tipple B (2005). Marked decline in atmospheric carbon dioxide concentrations during the Paleogene. Science 309: 600-603.

Pearson PN, McMillan IK, Wade BS, Jones TD, Coxall HK et al. (2008). Extinction and environmental change across the Eocene-Oligocene boundary in Tanzania. Geology 36: 179-182.

Perinçek D (1991). Possible strand of the North Anatolian fault in the Thrace Basin, Turkey - An interpretation. AAPG Bulletin 75: 241-257.

Popov SV, Akhmetiev MA, Zaporozhets NI, Voronina AA, Stolyarov AS (1993). Evolution of Eastern Paratethys in the Late Eocene-Early Miocene. Stratigraphy and Geological Correlation 1: 10-39.

Popov SV, Antipov PM, Zastrozhnov SA, Kurina EE, Pinchuk NT (2010). Sea level fluctuations on the Northern shelf of the Eastern Paratethys in the Oligocene-Neogene. Stratigraphy and Geological Correlation 18: 200-224.

Popov SV, Rostovtseva YV, Pinchuk TN, Patina IS, Goncharova IA (2019). Oligocene to Neogene paleogeography and depositional environments of the Euxinian part of Paratethys in Crimean - Caucasian junction. Marine and Petroleum Geology 103: 163-175.

Popov SV, Rögl F, Rozanov AY, Steininger FF, Scherba IG et al. (2004). Lithological- paleogeographic maps of the Paratethys. Courier Forschungsinstitut Senckenberg 250: 1-46.

Powell AJ (1992). Dinoflagellate cysts of the Tertiary System. In: Powell AJ (editor). A Stratigraphic Index of Dinoflagellate Cysts. 1st ed. London, UK: Chapman & Hall, pp. 155-252.

Pross J (2001). Dinoflagellate cyst biogeography and biostratigraphy as a tool for palaeoceanographic reconstructions: an example from the Oligocene of western and northwestern Europe. Neues Jahrbuch für Geologie und PalaontologieAbhandlungen 219: 207-219.

Pross J, Brinkhuis H (2005). Organic-walled dinoflagellate cysts as paleoenvironmental indicators in the Paleogene; a synopsis of concepts. Palaontologische Zeitschrift 79: 53-59.

Pross J, Houben AJP, van Simaeys S, Williams GL, Kotthoff U et al. (2010). Umbria-Marche revisited: a refined magnetostratigraphic calibration of dinoflagellate cyst events for the Oligocene of the Western Tethys. Review and Palaeobotany and Palynology 158: 213-235.

Pross J, Schmiedl G (2002). Early Oligocene dinoflagellate cysts from the Upper Rhine Graben (SW Germany): paleoenvironmental and paleoclimatic implications. Marine Micropaleontology 45: 1-24.

Rögl F (1999). Mediterranean and Paratethys. Facts and hypotheses of an Oligocene to Miocene Paleogeography (Short Overview). Geologica Carpathica 50: 339-349.

Sachsenhofer RF, Popov SY, Akhmediev MA, Betchel A, Gratzer R et al. (2017). The type section of the Maikop Group (Oligocene-lower Miocene) at the Belaya River (North Caucasus): depositional environment and hydrocarbon potential. AAPG Bulletin 101: 289-319.

Sachsenhofer RF, Stummer B, Georgiev G, Dellmour R, Bechtel A et al. (2009). Depositional environment and hydrocarbon potential of the Oligocene Ruslar Formation (Kamchia depression; Western Black Sea). Marine and Petroleum Geology 26: 57-84.

Şafak Ü, Güldürek M (2016). The Ostracoda assemblage of the Eocene-Oligocene transition in northwestern Thrace: Kırklareli-Edirne area (northwestern Turkey). Journal of African Earth Science 117: 62-85.

Sakınç M (1994). Karaburun (İstanbul) denizel Oligosen'in stratigrafisi ve paleontolojisi. MTA Bülteni 116: 9-14 (in Turkish).

Sancay RH (2005). Palynostratigraphic and palynofacies investigation of the Oligocene-Miocene units in the Kars-Erzurum-Muş sub-basins (Eastern Anatolia). PhD, Middle East Technical University, Ankara, Turkey.

Schouten S, Eldrett J, Greenwood DR, Harding I, Baas M et al. (2008). Onset of long-term cooling of Greenland near the Eocene-Oligocene boundary as revealed by branched tetraether lipids. Geology 36: 147-150.

Schulz HM, Bechtel A, Rainer T, Sachsenhofer RF, Struck U (2004). Paleoceanography of the western central Paratethys during Early Oligocene nannoplankton zone NP23 in the Austrian Molasse Basin. Geologica Carpathica 55: 311-323.

Schulz HM, Bechtel A, Sachsenhofer RF (2005). The birth of the Paratethys during Early Oligocene: from Tethys to a Black sea analogue. Global and Planetary Change 49: 163-176.

Şengör AMC, Yılmaz Y (1981). Tethyan evolution of Turkey: a plate tectonic approach. Tectonophysics 75: 181-241.

Shikhlinsky S, Batı Z (2008). Late Eocene-Early Oligocene Litho-biostratigraphy of the Caspian and Black Sea regions. In: EAGE International Conference on Petroleum Geology and the Hydrocarbon Potential of the Caspian and Black Sea Regions, 6–8 October, Baku, Azerbaijan.

Simmons MD, Bidgood MD, Connell PG, Coric S, Okay AI et al. (2020). Biostratigraphy and paleoenvironments of the Oligocene succession (İhsaniye Formation) at Karaburun (NW Turkey). Turkish Journal of Earth Sciences 29: 28-63.

Siyako M (2006). Trakya havzası Tersiyer kaya birimleri, In: Trakya Bölgesi Litostratigrafi Birimleri. Litostratigrafi Birimleri Serisi-2. Ankara, Turkey: MTA, pp. 43-83 (in Turkish).

Sliwinska KK, Heilmann-Clausen C (2011). Early Oligocene cooling reflected by the dinoflagellate cyst *Svalbardella cooksoniae*. Palaeogeography, Palaeoclimatology, Palaeoecology 305: 138-149.

Sluijs A, Pross J, Brinkhuis H (2005). From greenhouse to icehouse; organic-walled dinoflagellate cysts as paleoenvironmental indicators in the Paleogene. Earth Science Reviews 68: 281-315.

Soliman A (2012). Oligocene dinoflagellate cysts from the North Alpine Foreland Basin: new data from the Eggerding Formation (Austria). Geologica Carpathica 63: 49-70.

Sotak J (2010). Paleoenvironmental changes across the Eocene-Oligocene boundary: insights from the Central-Carpathian Paleogene Basin. Geologica Carpathica 61: 393-418.

Stolyarov AS, Ivleva EI (1999). Solenovian Rocks of the Lower Oligocene in the Ciscaucasia, Volga-Don, and Mangyshlak Regions (Central Part of the Eastern Paratethys): Communication 1. Main lithological and structural features. Lithology and Mineral Resources 34: 259-276

Stover LE, Brinkhuis H, Damassa SP, de Verteuil L, Helby RJ et al. (1996). Mesozoic–Tertiary dinoflagellates, acritarchs and prasinophytes. In: Jansonius, J, McGregor, DC (editors). Palynology: Principles and Applications 2. College Station, TX, USA: American Association of Stratigraphic Palynologists, pp. 641-750.

Torricelli S, Biffi U (2001). Palynostratigraphy of the Numidian flysch of North Tunisia (Oligocene–Early Miocene). Palynology 25: 29-55.

Tulan E, Sachsenhofer RF, Tari G, Flecker R, Fairbank V et al. (2020). Source rock potential and depositional environment of Lower Oligocene rocks in the Karaburun area, Turkey. Turkish Journal of Earth Sciences 29: 64-84.

Turgut S, Eseller G (2000). Sequence stratigraphy, tectonics and depositional history in eastern Thrace Basin, NW Turkey. Marine and Petroleum Geology 17: 61-100.

Turgut S, Türkaslan M, Perinçek D (1991). Evolution of the Thrace sedimentary basin and its hydrocarbon prospectivity. In: Spencer AM (editor). Generation, Accumulation, and Production of Europe's Hydrocarbons. Oxford, UK: Oxford University Press, pp. 415-437.

Van Couvering J, Aubry JA, Berggren WA, Bujak JP, Naeser CW et al. (1981). The Terminal Eocene Event and the Polish connection. Palaeogeography, Palaeoclimatology, Palaeoecology 36: 321-362.

Van Mourik CA, Brinkhuis H (2005). The Massignano Eocene-Oligocene golden spike section revisited. Stratigraphy 2: 13-30.

Van Mourik CA, Brinkhuis H, Williams GL (2001). Mid-to Late Eocene organic-walled dinoflagellate cysts from ODP Leg 171B, offshore Florida. Geological Society of London Special Publications 183: 225-251.

Van Simaeys S, De Man E, Vandenberghe N, Brinkhuis H, Steubaut E (2004). Stratigraphic and palaeoenvironmental analysis of the Rupelian–Chattian transition in the type region: evidence from dinoflagellate cysts, foraminifera and calcareous nannofossils. Palaeogeography, Palaeoclimatology, Palaeoecology 208: 31-58.

Van Simaeys S, Munsterman D, Brinkhuis H (2005). Oligocene dinoflagellate cyst biostratigraphy of the southern North Sea Basin. Review of Palaeobotany and Palynology 134: 105-128.

Varentsov IM (2002). Genesis of the eastern Paratethys manganese ore giants. Impact of events at the Eocene/Oligocene boundary. Ore Geology Reviews 20: 65-82.

Varentsov IM, Muzyliov NG, Nikolaev VG, Stupin SI (2003). The origin of black shale-hosted Mn deposits in Paratethyan basins: constraints from geological events at the Eocene/Oligocene boundary. Russian Journal of Earth Sciences 5: 255-272.

Williams GL, Brinkhuis H, Pearce MA, Fensome RA, Weegink JW (2004). Southern Ocean and global dinoflagellate cyst events compared; index events for the late Cretaceous–Neogene. In: Exon NF, Kennett JP, Malone MJ (editors). Proceedings of the Ocean Drilling Program, Scientific Results 189. College Station, TX, USA: Ocean Drilling Program, pp. 1-98.

Wilpshaar M, Santarelli A, Brinkhuis H, Visscher H (1996). Dinoflagellate cysts and mid-Oligocene in the central Mediterranean region. Journal of the Geological Society of London 153: 553-561.

Yancey TE, Elsik WC, Sancay RH (2002). The palynological record of late Eocene climate change, northwest Gulf of Mexico. Chapter 14. In: Prothero DR, Ivany LC, Nesbitt EA (editors). From Greenhouse to Icehouse: The Marine Eocene-Oligocene Transition. New York, NY, USA: Columbia University Press, pp. 252-268.

Yücel AO, Özcan E, Erbil Ü (2020). Latest Priabonian larger benthic foraminiferal assemblages at the demise of the Soğucak Carbonate Platform (Thrace Basin and Black Sea shelf, NW Turkey): implications for shallow marine biostratigraphy. Turkish Journal of Earth Sciences 29: 85-114.

Zachos JC, Pagani M, Sloan L, Thomas E, Billups K (2001). Trends, rhythms, and aberrations in global climate 65 Ma to present. Science 292: 686-693.

Zachos JC, Stott LD, Lohmann KC (1994). Evolution of early Cenozoic marine temperatures. Paleoceanography 9: 353-387.

Zaporozhets NI (1999). Palynostratigraphy and Dinocyst Zonation of the Middle Eocene-Lower Miocene Deposits at the Belaya River (Northern Caucasus). Stratigraphy and Geological Correlation 7: 161-178.

Appendix.

PALYNOMORPHS & SAMPLES, SECTIONS & PERCENTAGES		176	172	171	72	73	75	76	42	38	35	5	4
		Karaburun (2)	Karaburun (1)		Servez Beach				Servez Road Dam			Sazlıbosna	
DINOFLAGELLATE - ACRITARCH	*Achomosphaera alcicornu*	1.28		3.77					1.43			1.45	
	Achomosphaera sp.	1.28	1.02								27.27	0.58	1.81
	Areoligera semicirculata		5.10	1.24								0.58	
	Areoligera senonensis					3.03				3.86			
	Areoligera sp.	2.56	5.10				2.00					0.29	1.81
	Areoligera tauloma-sentosa											0.29	
	Areosphaeridium diktyoplokum									1.94		0.29	
	Areosphaeridium michoudii											0.58	
	Areosphaeridium multicornata							0.82	0.71			1.45	1.81
	Areosphaeridium sp.							0.27		9.94			
	Ascostomocystis potana	1.28							0.71				
	Batiacasphaera sp.	1.28									18.18		
	Charlesdowniea clathrata							0.82				1.16	
	Cleistosphaeridium placacanthum	10.26	8.16	2.48					0.71				
	Cleistosphaeridium sp.							0.82	2.86				
	Cordosphaeridium cantharellus	1.28		6.24				0.82	4.29	3.86		1.45	1.81
	Cordosphaeridium funiculatum	2.56	3.06			3.03		4.91	11.88				26.95
	Cordosphaeridium minimum											0.29	
	Cordosphaeridium sp.		1.02					0.27					
	Cribroperidinium sp.								7.04				
	Cyclopsiella lusatica					3.03		0.55					
	Dapsilidinium simplex											0.29	
	Deflandrea granulosa			3.77						1.98			
	Deflandrea leptodermata											0.87	

Appendix. (Continued).

DINOFLAGELLATE - ACRITARCH	*Deflandrea phosphoritica*	5.13	1.02	3.77					1.43	3.86			
	Deflandrea sp.		1.02									0.58	1.81
	Distatodinium ellipticum			1.24								0.87	
	Distatodinium sp.												
	Enneadocysta pectiniformis	5.13	3.06	2.48				0.27	2.14		45.45	2.02	
	Exochosphaeridium bifidum											0.87	
	Glaphyrocysta semitecta							0.55	9.05				
	Helicosphaera sp.									1.94			
	Hemiplacophora semilunifera											0.29	
	Homotryblium conicum								0.71				
	Homotryblium floripes											0.58	3.69
	Homotryblium pallidum											1.45	
	Homotryblium plectilum	6.41	14.29	7.56		9.09	10.00	14.31	4.13	3.88		0.58	
	Hystrichokolpoma cinctum	1.28	2.04	1.24									
	Hystrichokolpoma sp.								0.71				
	Hystrichostrogylon membraniphorum											0.29	
	Impagidinium dispertitum		2.04	1.24								0.29	
	Impagidinium sp.			1.24									1.81
	Impagidinium velorum		1.02	1.24									
	Kisselovia sp.												5.48
DINOFLAGELLATE - ACRITARCH	*Lingulodinium machaerophorum*		1.02	3.77					0.71				
	Melitasphaeridium choanophorum		1.02	1.24				0.27					
	Membranophoridium aspinatum	1.28	2.04				2.00	0.27				3.18	
	Membranophoridium connectum											0.58	
	Membranophoridium intermedium											0.29	
	Oligokolpoma galeottii	3.85					2.00	0.27				0.87	
	Oligosphaeridium complex							0.27	2.14	8.22			
	Operculodinium divergens												3.69
	Operculodinium microtriainum	5.13					8.00	1.09	9.87	1.94		0.58	1.81
	Operculodinium sp.			3.77									
	Palaeocystodinium sp.								0.71				
	Pentadinium laticinctum							1.64					
	Pentadinium sp.						2.00					1.45	1.81
	Phthanoperidinium comatum								2.14				
	Phthanoperidinium sp.							0.27	0.71				
	Polysphaeridium sp.	3.85	3.06	3.77	4.17				1.43				5.48
	Polysphaeridium zoharyii	2.56				3.03	8.00			8.14			
	Reticulatosphaera actinocoronata			1.24								0.29	
	Rhombodinium perforatum											0.29	
	Samlandia sp.	1.28							0.71			0.29	
	Spiniferites membranaceous		1.02										

Appendix. (Continued).

DINOFLAGELLATE - ACRITARCH	*Spiniferites mirabilis*	1.28											
	Spiniferites pseudofurcatus			5.02								0.29	
	Spiniferites ramosus	1.28	1.02	2.48									3.69
	Spiniferites sp.	2.56	2.04	3.77								0.87	1.81
	Stoveracysta ornata											0.58	
	Tectatodinium sp.											0.29	
	Thalassiphora pelagica							1.37	0.71				
	Undetermined dinoflagellate	1.28	1.02	1.24					3.57		9.09	0.87	1.81
	Wetzeliella gochtii		2.04	2.48			2.00	2.19					
	Wetzeliella sp.	1.28		1.24				7.82	3.57			0.29	
	Wetzeliella symmetrica		1.02	1.24				2.46					
SPORE - POLLEN - FUNGI	*Baculatisporites gemmatus*		1.02					3.25				1.16	5.48
	Carya			1.24									
	Cicatricosisporites dorogensis							0.82					
	Cingulatisporites macrospecious	2.56	1.02	2.48	8.33	9.09	2.00	3.28				0.58	5.48
	Corylus									1.94			
	Dicellaesporites sp.		1.02										
	Diporicellaesporites sp.												1.81
	Echinatisporis sp.		1.02	1.24				0.55				0.29	
SPORE - POLLEN - FUNGI	*Engelhardia*		1.02		12.50	3.03		1.91		6.06			
	Ephedripites sp.	1.28											
	Ericaceae							0.82					
	Hypoxilonites sp.			1.24									
	Laevigatosporites haardtii				4.17	3.03						0.29	
	Leiotriletes adriennis	1.28			8.33		4.00	1.37				0.29	
	Leiotriletes sp.									1.94			
	Leiotriletes dorogensis							0.27	0.71				
	Lusatisporites perinatus							1.37					1.81
	Multicellaesporites sp.					3.03							
	Periporopollenites multiporatus								0.71				
	Pityosporites spp.	5.13	6.12	3.77	12.50	9.09	18.00	33.92	6.88	14.32			
	Pluricellaesporites vermiculus	3.85											
	Pluricellaesporites sp.		2.04	1.24									
	Quercus	2.56	3.06		33.33	42.42	8.00	7.65	14.74	20.36			5.48
	Slowakipollis hippophaeoides					3.03		0.27					
	Sparganiaepollenites sp.								0.71	1.94			
	Schizosporis sp.											64.74	
	Tsuga				4.17								
	Trichothyrites sp.		1.02										
	Verrucatosporites alienus	1.28	1.02	3.77								0.29	
	Verrucatosporites favus	1.28		2.48			2.00	0.55	2.14			0.58	5.48
OTHERS	Foraminiferal linings	12.82	13.27	8.76	8.33	6.06	12.00	0.55		1.94		2.31	3.69
	Scolecodont	2.56	3.06		4.17		18.00	0.55		1.94		0.58	
	Tasmanites			3.77				0.27				0.58	3.69
	TOTAL COUNTS	78	98	83	24	33	50	368	146	49	11	347	55